

Variable Stars in the Open Cluster NGC 7142

Eric L. Sandquist, Andrew W. Serio¹

San Diego State University, Department of Astronomy, San Diego, CA 92182

`erics@mintaka.sdsu.edu, aserio@gemini.edu`

Matthew Shetrone

University of Texas, McDonald Observatory, HC75 Box 1337-L Fort Davis, TX, 79734

`shetrone@astro.as.utexas.edu`

ABSTRACT

We present new discoveries of variable stars near the turnoff of the old open cluster NGC 7142. Contrary to previous studies, we detect eight contact or near contact eclipsing binaries (including three near the cluster turnoff), and most of these have good probability of being cluster members. We also identified one long-period variable that resides far to the red of the cluster giant branch, and four new detached eclipsing binaries.

We have re-examined the question of distance and reddening for the cluster, and find that the distance is larger and reddening lower than in most previous studies. In turn this implies that NGC 7142 is probably slightly younger than M67, about 3 Gyr old. With an age of this size, NGC 7142 would be one of a small group of clusters with main sequence turnoff stars at the transition between convective and radiative cores.

Subject headings: binaries: general — binaries: close — binaries: eclipsing — stars: variables: general — open clusters and associations: general — open clusters and associations: individual (NGC 7142)

1. Introduction

Star clusters have long been testbeds for our understanding of the evolution of stars, the physics of the gas in their interiors, and the dynamics of the member stars. Variable

¹Current address: Gemini Observatory, Southern Operations Center, AURA, Casila 603, La Serena, Chile

stars can provide a great deal of additional information that allows us to tighten the screws on theoretical models attempting to predict cluster stellar characteristics from first principles. Pulsating stars can provide information about internal structure and stellar mass. Short-period semi-detached and contact binaries may contain encoded information about the dynamical history of the cluster. But perhaps most valuable of all are detached eclipsing binaries because they can provide high precision measurements of masses and radii for individual stars with a minimum of theoretical interpretation.

Variability studies of NGC 7142 have previously been carried out by Crinklaw & Talbert (1991) and Rose & Hintz (2007). Rose & Hintz searched for low-amplitude variables on a single night of observations, finding eight stars with significant light variations. Crinklaw & Talbert expected to find a number of short-period variable stars based on discoveries in clusters like NGC 188. V375 Cep was the only variable star they discovered in the cluster, although they lacked sufficient observations to determine a period. The variable is of interest because its photometry puts it very close to the turnoff of the cluster’s color-magnitude diagram, within the main sequence band. Masses for these stars would be valuable constraints on the cluster age, but in addition, one of the two stars could be significantly evolved from the zero-age main sequence. This means that the radius of the star could help refine the age of the cluster. [One other semi-regular variable, V582 Cep, was known (Lasker et al. 1990) to be in the field of the cluster, but was outside the field observed by us.

In one of the earliest studies of the cluster, van den Bergh & Heeringa (1970) found that NGC 7142 was intermediate in age between NGC 7789 and M67, approximately 1.5 – 4 Gyr. Crinklaw & Talbert (1991) found that it was intermediate in age between M67 and NGC 188, or approximately 4 – 5 Gyr. Carraro et al. (1998) estimated an age of 4.9 Gyr by comparing synthetic color-magnitude diagrams (generated from model isochrones) with photometry. Salaris et al. (2004) give an age of 4 ± 1 Gyr for NGC 7142 based on the magnitude difference between the subgiant branch and the red giant clump. Recently though, Janes & Hoq (2011) derived a much larger age of 6.9 ± 0.8 Gyr, using synthetic CMDs to match the turnoff color and red giant clump color and magnitude. Much of the disagreement may be the result of differential extinction in the cluster and the small numbers of evolved stars, making the reference points in the CMD difficult to identify.

In order to improve the precision of the age determination for this old open cluster (and others), we have undertaken a program to identify and analyze age-sensitive eclipsing binary stars. This paper presents the results of our variable search, and a following study presents and analysis of the most promising candidates.

2. Observational Material and Data Reduction

2.1. Photometry

All of the photometry for this study was taken with the Mount Laguna Observatory 1 m telescope using a camera having a 2048×2048 pixel CCD and approximately a $13'.5 \times 13'.5$ field of view. Table 1 lists the nights during which images were taken for this article. 17 nights of data were taken in R_C band for the purpose of identifying variable stars in the cluster, and subsequent nights were taken primarily to refine the ephemerides of the most important variables and to determine light curves in different filter bands.

Differential photometry was undertaken using the image subtraction package ISIS (Alard 2000). Our procedure is very similar to that of Talamantes et al. (2010), so for most details, we refer the reader to that paper. Our image sets in B , V , R_C , and I_C filters were interpolated to a common image coordinate system, and then processed separately by filter.

The output of ISIS is a difference flux measured on the subtracted images. To convert these difference fluxes into magnitudes, star fluxes were measured on the reference frame. ISIS’s algorithm is a modified aperture photometry routine that employs the reference image point-spread function (PSF) for weighting purposes. The reference PSF is first transformed to the seeing of the image under consideration. Only the portion within an aperture of `radphot` pixels will be used, but it is normalized to a larger aperture of `rad_aper` pixels. The pixel values in the subtracted image are weighted by this transformed PSF. In this study, we used `radphot` = 4 pix and `rad_aper` = 10 pix.

We discovered a bug in the determination of uncertainties in the difference fluxes derived by ISIS. As part of the image subtraction process, the overall flux scaling from frame to frame is fit and corrected in ISIS. This scaling affects the size of the noise and therefore the flux uncertainties, but this was not done in the last version of ISIS. This had the unfortunate effect of depressing computed uncertainties on measurements with low fluxes. We fixed this error in our copy of the ISIS code (version 2.2), and all of the results here use this corrected version.

2.1.1. Photometric Calibration

We took calibration images under photometric conditions on the night of 25 October 2008. We observed the standard fields PG0231+051, SA 92, SA95, SA 98, and NGC 6940, and used standard values taken from Stetson (2000, retrieved August 2009). The standard fields were observed between 3 and 10 times per filter in BVI at airmasses that ranged from

1.034 to 1.998. All together this resulted in more than 4000 standard star observations per filter covering a color range $-0.5 \lesssim (B - I) \lesssim 5$.

We derived aperture photometry from all frames using DAOPHOT, and made curve of growth corrections using the program DAOGROW. The observations were transformed to the standard system using the following equations:

$$b = B + a_0 + a_1(B - I) + a_2X$$

$$v = V + b_0 + b_1(B - I) + b_2X$$

$$i = I + c_0 + c_1(B - I) + c_2X$$

where b , v , and i are instrumental magnitudes, B , V , and I are standard-system magnitudes, X is airmass, and a_i , b_i , and c_i are coefficients determined from least-squares fits. Fig. 1 shows the residuals of the comparison of our standardized observations and the Stetson values.

Clusters to be calibrated were observed with a range of exposures times on the same night. For NGC 7142, there were 9 observations in B (1×60 s, 5×120 s, and 3×300 s), 8 observations in V (3×60 s, 2×120 s, and 3×300 s), and 11 observations in I (4×10 s, 2×60 s, 2×120 s, and 3×300 s).

Little attention had been paid to NGC 7142 in the past, with Crinklaw & Talbert (1991) providing the most extensive set of photometry. Fig. 2 shows a comparison of our photometry with theirs. There are small zeropoint differences between the two studies, but more importantly, there is a clear trend with color. We believe our calibration is superior based on number of standards and improved technique. We have also compared to the more recent photometry by Janes & Hoq (2011). The zeropoint differences are again small as shown in Fig. 3, but there are also no obvious trends with color.

The color-magnitude diagram for our field is shown in Fig. 4. Note that much of the scatter probably comes from differential reddening resulting from the cluster’s proximity on the sky to the reflection nebula NGC 7129 (although the cluster is well behind the cloud). However, to help identify the cluster’s sparsely populated giant branch, we identified all the stars with radial velocities from spectra that have been presented in the literature (Friel & Janes 1993; Jacobson et al. 2007, 2008).

2.2. Spectra

Spectra for three variable star targets and three red clump star candidates were obtained at the Hobby-Eberly Telescope (HET) with the High Resolution Spectrograph (HRS, Tull

1998) as part of normal queue scheduled observing (Shetrone et al. 2007). The observed stars are listed in Table 2. HRS was configured to HRS_30k_central_316g5936_2as_0sky_IS0_GC0_2x3 or HRS_30k_central_600g5822_2as_2sky_IS0_GC0_2x3 to achieve $R=30,000$ spectra covering 4100Å to 7800Å or 4825Å to 6750Å respectively. Exposure times ranged from 600 seconds to 1200 seconds. The signal-to-noise was typically 25 per resolution element at 5800 Å.

The spectra were reduced with IRAF ECHELLE scripts. The standard IRAF scripts for overscan removal, bias subtraction, flat fielding and scattered light removal were employed. For the HRS flat field we masked out the Li I, H I and Na D regions because the HET HRS flat field lamp suffered from faint emission lines. The spectra were combined into a single long spectrum for the blue and red chips. Radial velocities were determined from cross-correlation using the IRAF task `fxcor` using the solar spectra. The heliocentric correction was made using the IRAF task `rvcorrect`. The radial velocities are discussed in more detail in §3.2.

3. Variable Stars

We present the detected variable stars in Table 3. We have started a new nomenclature for all detections (except the one known variable V375 Cep), ordered by V magnitude. Rose & Hintz (2007) identified 8 stars as “suspected” variable stars and an additional 12 as “potential” (less likely) variables. Even though all of their systems were in our field and all but five were faint enough to be within the dynamic range of our images, only two of the stars in their list were identified as variables in our observations.

3.1. Contact and Near-Contact Binaries

Because our calibration observations were taken over two relatively short periods on one night, we determined corrections to the calibrated magnitudes for each of our close binary systems to give us values at maximum light. These corrections were as large as about 0.1 mag in a few cases, which is enough to affect judgements about cluster membership from CMD position.

Short-period contact and near-contact binary star systems have only been found in open clusters older than about 600 Myr (Rucinski 1998; Zhang et al. 2009). For fainter systems, this comes about as a result of the long timescales for tidal interactions to produce orbital decay. At the bright end though, the evolution of one component of a binary can accelerate the process. NGC 7142 has 4 contact or near-contact systems near the cluster

turnoff, comparable in number to systems fainter on the main sequence. Similar groupings of systems are seen in old open clusters like M67 (Sandquist & Shetrone 2003) and NGC 7789 (Jahn et al. 1995), supporting the idea that mass transfer (and potentially coalescence of the stars) can produce blue straggler stars. This does not appear to be universal among open clusters, however. Rucinski (1998), for example, found that such systems are not concentrated at the turnoff, but can be found spread brightward (among blue stragglers) or faintward (along the main sequence).

Before drawing conclusions, we can assess whether the contact binaries are likely to be members using the period-luminosity-color (PLC) relationship from Rucinski & Duerbeck (1997)

$$M_V = -4.44 \log P + 3.02(B - V)_0 + 0.12$$

and comparing the implied distance modulus to what is estimated from isochrones. The significant differential reddening in NGC 7142 will reduce the sharpness of this tool by introducing additional random scatter of approximately 0.15 mag, but in some cases we should be able to make strong statements. Based on our later discussion of the red giant clump (§4.2 and 4.3), we find that the mean reddening for the cluster appears to be $E(B - V) \approx 0.36$, with a distance modulus $(m - M)_V = 13.18$. V5 has an implied distance modulus about 2 mag smaller $[(m - M)_V = 11.1]$, and V13 has a value almost a magnitude larger (14.0). Two of the remaining systems are very consistent with cluster membership (V3: 13.1; V9: 13.0), while two others are possible members (V7: 13.5; V12: 13.4). Because NGC 7142 is similar in age to other clusters (such as M67) known to have contact binary members, these new detections are understandable, although the systems don’t seem to show any sign of being concentrated toward the cluster center.

V3 (Fig. 5): This is one of the systems that was “suspected” to be variable by Rose & Hintz (2007) that we confirm as variable (their star 279). Based on the PLC relation, this system may be a cluster blue straggler. There are slight but distinct differences between the depths of the two eclipses, and there are also signs of light curve variability in the R data (which covers the largest range of time) on a timescale of weeks. Strangely, these light curve variations seem to primarily affect the maxima and minima.

V5 (Fig. 5): This is a “potential” variable previously identified by Rose & Hintz (2007) that we confirm here (their star 170). The depths of the eclipses in different bands differ significantly, with eclipses getting deeper for bluer filter bands. In other close binaries, this might imply light curve variability, yet we don’t see strong evidence of this. V5 is interesting because it is quite red compared to the main sequence, but falls very near the base of the giant branch. However, the PLC relation implies that this is probably a foreground system.

V6 and V7 (Figs. 6 and 7): Both of these systems fall very close to the cluster

turnoff, and their variability may be related to evolution-driven size changes if they turn out to be cluster members. The eclipses for V6 have very different depths (~ 0.42 mag versus 0.19 mag in R) indicating that the stars are close, but probably not in physical contact. As a result, the two stars may not have exchanged significant amounts of mass and the mass of the primary star may be a future constraint on the cluster age.

V7 is probably a W UMa-type variable with a low inclination. The light curve shows an amplitude of about 0.02 mag as well as hints that the photometric minimums have different depth. A period of about 0.695 d seems to be preferred, but cycle-to-cycle variability interferes with a definitive determination of the ephemeris.

V9 (Fig. 5): This system has fairly deep eclipses that are similar in depth. The combined photometry places it to the red of the main sequence but near the expected location of the equal-mass binary sequence.

V12 (Fig. 5): This object is toward the faint end of our sample, and its amplitude is small and possibly variable. The system does fall near the main sequence in the CMD though. It is difficult to find a period under those conditions, but a period of approximately 0.29 d appears to be the best job of phasing the observations.

V13 (Fig. 5): V13 appears to show a total eclipse, making a membership determination of interest. V13’s corrected system photometry places it close to the cluster main sequence, although this portion of the CMD is fairly heavily contaminated by the field star population. The distance modulus derived from the PLC relationship is almost a magnitude greater than estimates for the cluster, making it unlikely to be a member. The system shows clear variability from night to night. The most notable example occurred during a 10 day break in observations in R when the system’s median value dropped by approximately 0.04 mag. During the course of the observations in R , the light curve maxima varied over a range of about 0.10 mag.

V14 (Fig. 5): This is the faintest of the near-contact systems, and it also showed significant changes in brightness and amplitude over the course of 2 months of observations in R . There appeared to be some correlation between eclipse depth and the brightness level at the quadratures.

3.2. Detached Eclipsing Binaries

Using spectroscopic data for three of the detached eclipsing systems (V1, V2, and V375 Cep), we simultaneously determined the center-of-mass radial velocity and the mass ratio by

χ^2 minimization of a conservation of momentum condition. For all measured radial velocity pairs, we minimized

$$\sum (v_A - v_{CoM} + q(v_B - v_{CoM}))^2 / (\sigma_A^2 + \sigma_B^2)$$

The results are shown in Table 2.

There has been relatively little radial velocity work done on NGC 7142 that can be used to judge the membership of the measured stars. Friel et al. (1989) measured radial velocities for 13 stars in the field of the cluster using relatively low-resolution spectra, finding a mean value of -44 km s^{-1} (12 km s^{-1} standard deviation, and typical measurement errors of $10 - 15 \text{ km s}^{-1}$). Jacobson et al. (2007) measured 6 stars and found $-48.6 \pm 1.1 \text{ km s}^{-1}$, while Jacobson et al. (2008) found $-50.3 \pm 0.3 \text{ km s}^{-1}$ from higher resolution spectra of 4 of the same stars. If NGC 7142 is still in virial equilibrium, the cluster velocity dispersion should be small ($\lesssim 1 \text{ km s}^{-1}$) given likely masses for the cluster (Piskunov et al. 2008, e.g.). However, the number of stars with high precision radial velocities is still small and the distribution of field stars has not been characterized, so membership judgements using the radial velocities should still be made with care.

V1 (Fig. 8): Primary and secondary eclipses were initially detected with comparable depths, making this very likely to be a double-lined spectroscopic binary with stars of comparable mass. We subsequently confirmed two detectable components in spectra taken with the HET. Although the system falls in the blue straggler portion of the color-magnitude diagram, there was a possibility that the components are main sequence stars because differential reddening may affect the position of the blend in the CMD. Our three radial velocities imply a mass ratio $q = 0.96 \pm 0.02$ and a system velocity $v_r = -17.0 \pm 1.0 \text{ km s}^{-1}$. The system velocity puts it far away from the likely cluster mean. Based on the small displacement of the secondary eclipse from phase 0.5, the binary also has at least a small eccentricity. Binaries with periods this short ($< 5 \text{ d}$) appear to be able to circularize on timescales much shorter than NGC 7142’s age (Meibom & Mathieu 2005), although on its own this is not conclusive because some known blue stragglers have short periods and significant eccentricity. But based on these indications, we conclude it is most likely not a member of the cluster.

V2 (Fig. 9): This appears to be a rather extraordinary eclipsing binary system. It was first identified in a single deep ($\sim 0.75 \text{ mag}$) eclipse in our observations from 2005. While characterizing the light curve of V375 Cep (see below) in 2008, we detected two additional eclipses (a primary and a secondary) separated by about 19.03 d. At that time, we noticed that the secondary eclipse ingress was significantly longer in duration than the primary eclipse, implying a significant eccentricity. However, the large separation between the first and second observed eclipses (1017.3 d) in combination with the eccentricity made it difficult to determine the period. Using the photometric constraints along with three

subsequent radial velocity measurements, we were able to narrow down the possibilities by requiring i) no photometric observations at constant light overlapped with predicted eclipses, and ii) radial velocities should have a physically realistic distribution in phase (e.g., no sudden changes in direction implied when phased). Using these constraints, the system was observed on dates with eclipses predicted for the most likely periods until a period of 15.6505 days was finally confirmed.

With this period, the secondary eclipse is centered near phase $\phi = 0.22$, consistent with a large eccentricity. The spectra of the system to date confirm that it is double-lined and that the system velocity ($-42.1 \pm 0.6 \text{ km s}^{-1}$) falls near the mean cluster value, but different by about several km s^{-1} . At this time, we have to regard V2 as a possible cluster member. In spite of the measured mass ratio ($q = 0.99 \pm 0.10$), the two stars differ significantly in size, showing the effects of evolution. When the depths of the eclipses are considered, the implied inclination of the orbit is very close to 90° .

In the CMD, V2 falls in the blue straggler region, brighter and bluer than the turnoff. Both of the stars individually have magnitudes placing them near the turnoff, and one or both may still be bluer than the turnoff when their light is disentangled. At this time, however, we cannot rule out the possibility that they are on a line of sight having less than the average cluster reddening. The characteristics of the orbits in V2 don't appear to distinguish between these possibilities: the period at which most binaries have circularized in M67 (which has similar age to NGC 7142) is approximately $12.1^{+1.0}_{-1.5} \text{ d}$ (Meibom & Mathieu 2005).

V375 Cep (Fig. 10): This system was the primary motivation for many of the observations we took, and so we have observations of primary and secondary eclipses in all photometric bands. The secondary eclipse is clearly detected, and we have shown that it is a double-lined spectroscopic binary. The spectroscopic data give $v_{CoM} = -49.1 \pm 1.7 \text{ km s}^{-1}$ and $q = 0.69 \pm 0.03$, and a minimum $\chi^2_\nu = 0.98$. v_{CoM} is completely consistent with the cluster average (see the beginning of this section), making it a highly probable cluster member.

We collected a small number of previous photometric observations from Crinklaw & Talbert (1991) and Seeberger et al. (1991) to improve the accuracy of the ephemeris and test for the possibility of a nonlinear ephemeris using the 27 y baseline. For the densely observed light curves from our study, we used the method of Kwee & van Woerden (1956) to determine times of minima and the errors.

Most of the observations by Crinklaw & Talbert (1991) agree well with our phased light curve and confirm that they observed the system very near one of the primary minima. They had observations in and out of eclipse on the night of one eclipse, which allowed us

to fit our BV light curves to their data and derive an approximate time of minimum. One additional observation in V on a different date also appears to have fallen near an eclipse minimum. If there are no errors in their Table 2, the separation between their two faintest measurements in V (26.83 d) would be consistent with a period of about 1.91647 d. However, the implied change in period over the 20 years since the Crinklaw & Talbert observations seems unrealistically large. A linear ephemeris that satisfactorily matches our data and one of the Crinklaw & Talbert eclipse observations would cause a disagreement of about 0.06 in phase for the other, which is slightly longer than the entire duration of an eclipse ingress.

In addition, most of the Seeberger et al. eclipse measurements disagree significantly with a linear ephemeris based on our data. They appear to have caught three measurements during the egress of a primary eclipse on one night (HJD 2446650), although the steeper slope and larger depth of their eclipse of when compared to ours makes it hard to trust estimations of the time of minimum. We have therefore elected to assign asymmetric error bars to that point. Two faint measurements in B seem likely to have been taken during ingress and egress respectively, if the period has remained near 1.9 d. However, another observation in B later on one of those nights was not consistent with out-of-eclipse levels or with predictions based on our eclipse light curves. Unfortunately it appears that the early data on this variable is not of sufficient quality to test for nonlinearities in the ephemeris.

V8 (Fig. 11): This is a binary with partial eclipses of quite small amplitude ($\sim 0.03 - 0.04$ mag). Eclipses were detected on some consecutive nights separated by about 1.0546 days, although we find the light curves phase together better when half this period is used. If the true period is indeed near 0.53 d, a secondary eclipse is not detected.

This system falls near the expected position of the equal-mass binary sequence, so it has a reasonable probability of cluster membership. However, if it is a cluster member, it would need to be a triple system, as this would explain both the shallow eclipses (through the diluting effects of third light) and the position in the CMD brighter than the main sequence. A third star with brightness similar to the primary of the binary system would need to be on a wider orbit. If the system is not a cluster member, it could involve a star being eclipsed by a smaller faint object. The significant out-of-eclipse variation implies that the companion must be of stellar mass in order to significantly distort the primary.

V11 (Fig. 12): Eclipses were detected in R at HJD 2453594.97, 2453598.83, 2453638.70, and 2453639.99, in V at 2454676.74, 2454678.02 (only ingress), and 2455081.93, and in B at 2454627.85. In two cases, eclipses of nearly equal depth (~ 0.2 mag) were observed on consecutive nights, and in one additional case, eclipses were separated by about 3.85 d. These observations make the period very likely to be near 1.3 d. Phasing the observations to this period, it appears we may have detected a shallow secondary eclipse in I band only,

centered at phase 0.5 with approximate depth 0.03 mag. This system is therefore likely to be a single-line spectroscopic binary with a fairly small mass ratio. Although we do not have radial velocity measurements for this system, the position of the system in the CMD implies that there is a good chance of cluster membership.

The primary eclipses appear to have a short period of totality. We also see strong out-of-eclipse light curve variations. For example, observations in 2005 separated by a little more than a month show large differences in the out-of-eclipse phases. In addition, a later night of observations in R shows the system brightness increasing before an eclipse, contrary to other observations at similar phase. The variations may be due to strong spot activity driven by rapid rotation in a system with such a short orbital period.

3.2.1. *Other Variables*

V4 shows variability on multiple timescales and with different amplitude. We have averaged measurements for each night in Fig. 13 to make these trends clearer. Because of the large numbers of observations, the errors in most of these averages are smaller than the sizes of the points. During individual nights of observation there are small but significant trends of about 0.01 mag, particularly noted in our B and V observations. On the other hand, our observations reveal longer timescale variations (tens of days) of greater amplitude (at least 0.6 mag in B , V , and R). Comparisons of observations of measurements in different filter bands should be regarded as approximate — the medians in each band generally do not correspond to the identical times in the oscillation cycle, and there is evidence that the variation amplitude varies from band to band.

V4 appears to be an single star in our best seeing images. The CMD position of the star sets it apart — it is quite red even for a star on the giant branch, and even accounting for realistic amounts of differential reddening. On the night of our calibration observations (HJD 2454765), the star appears to have been in a bright phase: more than 0.6 mag above the median of our B measurements, and about 0.2 mag above the median in V . (Note that we generally did not take observations in multiple bands during one night, so the median measurements are probably not representative of corresponding points in the variability cycle of the star.) However, V4 resides in a similar position in the CMDs of van den Bergh & Heeringa (1970, star Y) and Crinklaw & Talbert (1991). Our calibration observations and the observations of these other photometric studies were taken close together in time, so that they should be fairly representative of the object’s instantaneous color. Because they place the star to the red of the cluster giant branch, the calibrated color cannot be representative of a static star if it is a cluster member as it would be redder than

the Hayashi line.

The nature of the variability and its CMD position are somewhat reminiscent of two variable members of the similarly old cluster M67 (van den Berg et al. 2002; Sandquist & Shetrone 2003). S1063 and S1113 sit below the subgiant branch of M67 (Mathieu et al. 2003) and are both X-ray sources and spectroscopic binaries. S1113 shows fairly periodic variations, while S1063 does not. In both cases, the variations are of much smaller amplitude than we see in V4. We have not detected variability among stars below the subgiant branch in NGC 7142, and they would be impossible to identify based on CMD position alone, thanks to field star contamination. We also carefully examined the other object that resides near V4 in the CMD, but saw no sign of variability. Spectroscopic information would be valuable to verify the stellar nature of the star, to check cluster membership (both by measuring radial velocities and by checking the possibility that it is a background giant).

V10 appears to be a quasiperiodic variable. On any given night the star shows a trend in brightness of up to about 0.1 mag from beginning to end. Fig. 14 shows our observations in R_C , but similar variation appears in other filters as well. Using the Lafler-Kinman method (Lafler & Kinman 1965), we found the most likely periods of variability to be approximately 1.38 and 2.77 d, but we have not been able to find a period that phases all of the datasets satisfactorily. The object is well separated from other sources, so that contamination of the photometry is unlikely. Based on its CMD position redder than the equal-mass binary sequence, it is not likely to be a cluster member. However, its unusual variation may be worth further study.

4. Discussion

Overall, little work has been done on NGC 7142 compared to other open clusters, but as will be seen below, there is reason to believe the cluster’s characteristics should be revised. Before addressing the age of the cluster with a traditional isochrone fit, we first review previous estimates of the metallicity, distance, and reddening.

4.1. Metallicity

In the last decade or so, spectroscopic measurements of NGC 7142’s metallicity have been moving more metal-rich. This trend of cluster metallicities moving more metal-rich with time is not unique to this cluster (see Gratton et al. 2006 for NGC 6791, for example), but the fact that the cluster now seems to be slightly more metal-rich than the Sun is important

for accurate age determination. The first spectroscopic measurement for NGC 7142 by Friel & Janes (1993) ($[\text{Fe}/\text{H}] = -0.23 \pm 0.13$) as part of a larger survey of open clusters was later revised upward to -0.10 ± 0.10 by Friel et al. (2002) based on a new calibration of Fe spectroscopic indices. Twarog et al. (1997) computed an even higher value ($+0.04 \pm 0.06$) by transforming the same Friel & Janes (1993) data to a common metallicity scale based on DDO photometry. Later spectroscopic measurements ($+0.08 \pm 0.06$, Jacobson et al. 2007; $+0.14 \pm 0.01$ from 4 giants, Jacobson et al. 2008) also indicated a super-solar metallicity, however. NGC 7142 also appears to be more metal rich than the well-studied cluster M67 ($[\text{Fe}/\text{H}] = 0.00 \pm 0.09$, Twarog et al. (1997); $+0.03 \pm 0.07$, Friel et al. (2010)) in studies where the two clusters can be compared reliably.

4.2. Distance and Reddening

van den Bergh & Heeringa (1970) determined that the reddening for the cluster was $E(B - V) = 0.41$ using the UBV color-color diagram, and this has been the most commonly quoted value since. Crinklaw & Talbert (1991) found evidence of differential reddening on the order of $\Delta E(B - V) = 0.1$ based on the width of the observed main sequence. Even though there are clear signs of a cloud front stretching ENE to WSW (with the amount of gas appearing to decrease toward the SSE), Crinklaw & Talbert did not find evidence of a systematic change in reddening across the face of the cluster. They interpreted this to mean that there is significant smaller scale variation. Twarog et al. (1997) settled on $E(B - V) = 0.43$ for turnoff stars and 0.40 for giants, based on a survey of previous studies including the two above. Janes & Hoq (2011) derived $E(B - V) = 0.32 \pm 0.05$ using a method depending largely on comparing photometry of the red giant clump and main sequence turnoff to those of synthetic CMDs generated from isochrones. The reddening derived from IRAS and COBE dust maps (Schlegel et al. 1998) is significantly larger [$E(B - V) = 0.51 \pm 0.02$] than any previous determination for the cluster, but this might be a better indication of the reddening of stars beyond NGC 7142. The dust map values do vary in a range covering 0.09 mag within $5'$ of the cluster center, lending some credence to the possibility of differential reddening for the cluster.

There has not been much agreement among previous distance modulus determinations either. The first estimate by van den Bergh & Heeringa (1970) was $(m - M)_V \simeq 13.7$. Crinklaw & Talbert (1991) quoted a dereddened distance modulus $(m - M)_0 = 11.4 \pm 0.9$ when using $E(B - V) = 0.41$, corresponding to an uncorrected distance modulus of

⁰<http://irsa.ipac.caltech.edu/applications/DUST/>

approximately $(m - M)_V = 12.67$. Twarog et al. (1997) derive $(m - M)_V = 12.95$ from main sequence fitting, assuming $E(B - V) = 0.43$. Janes & Hoq (2011) derive $(m - M)_0 = 11.85 \pm 0.05$, or $(m - M)_V = 12.84$.

Given the disagreements, it is worth revisiting the issue here. Of the features in the CMD on NGC 7142, the red giant clump is probably the most clearly identifiable, and some stars within it have been identified spectroscopically as likely cluster members. We identified candidate clump stars in optical and 2MASS infrared CMDs (see Fig. 15), and the 6 stars are given in Table 4. Obviously, the sample is small, and there may be a field star or first-ascent giant star present, given the amount of differential reddening across the cluster’s face. In fact, one star (CT 399) was rejected based on radial velocity measurement (Jacobson et al. 2007). We obtained single radial velocity measurements for three other red clump stars (listed in Table 2), and one of them (JH 2222) is consistent with membership, while the other two have velocities that are separated from the cluster mean by $\sim 4 \text{ km s}^{-1}$ and whose memberships are still in question. However, by using the median magnitude and color of the sample in 2MASS photometry (as did Grocholski & Sarajedini 2002 in their study of open cluster clump stars), the problems related to membership determination should be minimized.

The color of the clump is largely a function of age in the range of composition containing NGC 7142 [$\partial(J - K_{BB})_0/\partial \log t_{age} \approx -0.17 \text{ dex}^{-1}$] according to the open cluster data of Grocholski & Sarajedini (2002). Based on their study, the clump is predicted to have a color $(J - K_{BB})_0 = 0.67 \pm 0.03$, where we have assumed an age similar to M67 (4 Gyr) with a conservative uncertainty of about 1.5 Gyr. For NGC 7142, we find a median observed color $(J - K_{BB}) = 0.80$, for a reddening $E(J - K_{BB}) = 0.13 \pm 0.03$ or $E(B - V) = 0.25 \pm 0.06$.

Using the median magnitude for NGC 7142 stars ($K_{BB} = 10.42$), and the median absolute value from Grocholski & Sarajedini for stars similar in age and metallicity to NGC 7142 ($\langle M_K \rangle = -1.62 \pm 0.06$), we find $(m - M)_K = 12.04 \pm 0.15$. These values imply $(m - M)_0 = 11.96$ or $(m - M)_V = 12.72 \pm 0.19$. The reader should note that the 6 most probable clump stars are separated into two groups in K magnitude and $(J - K)$ color, and the medians split the difference here. In the optical CMD used by Janes & Hoq (2011), there is a greater degree of consistency in the V magnitudes of the clump stars, which is somewhat odd considering the apparent differential reddening across the cluster.

After comparing with the results of previous studies, the two results derived from the clump (this study and that of Janes & Hoq) give the largest values for the distance and smallest values for the reddening (with the exception of the early estimates by van den Bergh & Heeringa 1970). Earlier estimates were probably affected by degeneracy between the effect of dust extinction and distance, particularly because other features (like the turnoff) are difficult to

identify in the cluster’s CMDs. The larger distance implies that the turnoff is more luminous than previously thought and that the age will tend to be on the low side, as discussed below.

4.3. Age

Part of the motivation for this project involved finding detached eclipsing binary star systems that contained evolved stars. Precise measurements of the masses and radii for stars that have evolved off the main sequence can lead to precise age determinations for the cluster. A detailed analysis of the two detached eclipsing binary systems sitting at the cluster turnoff (V375 Cep and V2) and the implications for the cluster age will be presented in an upcoming paper. However, it is beneficial to have as reliable an age determination from isochrones and the CMD for comparison.

With the current CMDs, it is not easy to tell whether NGC 7142 turnoff stars are high enough in mass to produce a significant “hook” feature associated with core convection on the main sequence. A detailed isochrone fit for a feature of that kind is complicated by the short evolution timescale for stars moving through the hook, and the difficulties are exacerbated by differential reddening across the face of the cluster, field star contamination, and confusion due to optical blends of stars or true binaries. There is a weak indication of a subgiant branch at $V \approx 15.8$, sloping faintward from the massive end of the main sequence, but more work is needed to establish the cluster membership of these stars.

As a first check, we compare with M67, a well-studied cluster with an age thought to be near that of NGC 7142 (van den Bergh & Heeringa 1970; Crinklaw & Talbert 1991). M67 has a low and well-determined reddening ($E(B - V) = 0.041 \pm 0.004$; Taylor 2007), and a well-determined distance modulus [$(m - M)_V = 9.72 \pm 0.05$, $(m - M)_0 = 9.60 \pm 0.03$; Sandquist 2004]. M67 also appears to be a transition object, with evidence of weak core convection for the most massive turnoff stars, and a sparsely populated subgiant branch.

Because photometry is available in BVI_C (Sandquist 2004) and JHK_S (Skrutskie et al. 2006), differences in median magnitudes of the clump of the clusters in different filters allow a good estimate of the difference in distance moduli. In the 2MASS filters where the effects of extinction are minimized, these differences converge to about 2.4 mag. With a small correction for the extinction, this implies $(m - M)_{0,N7142} - (m - M)_{0,M67} = 2.3$, and $(m - M)_0 = 11.9$. We can then look for consistency when the color-magnitude diagrams of the clusters are overlaid in different filter combinations in order to check the earlier estimate of the reddening. This requires that the extinctions and reddenings in different filter combinations can be reliably related, which is a complicated subject (McCall 2004). For example, the

measured reddening should depend on the spectral type of the star being observed because the flux-weighted wavelength of detected photons (the “effective wavelength”) changes. The use of Cardelli et al. (1989) extinction relationships (including the use of $R_V = A_V/E(B-V)$ values different from the canonical 3.1) did not produce consistent CMDs in optical bands. In Fig. 16, we show the results of using the method of McCall (2004) to compute reddenings and extinctions from $E(V-I)$, which was itself estimated from the shifts between the red clump stars in the two clusters and assuming the clump stars are approximately K1-K2 III giants. Calculations were done using the York Extinction Solver¹. As can be seen, the resulting CMDs show that the clumps, giant branch stars and main sequence lines largely agree in position.

The expected extinctions and reddening for turnoff stars (near F5 V) only differ from the clump values by 0.02 (in the optical) at most. So we conclude that differential effects due to the differing spectral energy distributions of giants and dwarfs are a minor effect on the quality of the fit.

Based on the comparison with M67, NGC 7142 appears to be a slightly younger cluster than M67. Even with some uncertainty in where to align the clumps of the two clusters, there is a group of NGC 7142 stars that reach up to about 0.75 mag brighter than the turnoff of M67. Using measured values for M67 and the results of the fit, our preferred values are $E(B-V) = 0.32 \pm 0.06$, $(m-M)_0 = 11.9 \pm 0.15$, and $(m-M)_V = 12.96 \pm 0.24$. The color difference between the turnoff and the giant branch is similar for the two clusters, although M67 has a larger difference in magnitude between the clump and the turnoff, implying that NGC 7142 is younger.

At the suggestion of the referee, we also compared NGC 7142 to the more metal-rich ($[\text{Fe}/\text{H}] = +0.43$; Anthony-Twarog et al. 2010) open cluster NGC 6253. If the NGC 6253 photometry is shifted [$\Delta V = 1.1$ mag, $\Delta(B-V) = 0.02$] so that the red clumps are once again in approximate agreement, the main sequences also agree as shown in Fig. 17. The brightness of subgiant star candidates in NGC 6253 indicate that that cluster is similar in age to or slightly younger than NGC 7142. Present indications are that NGC 6253 is around 3 Gyr old (see Montalto et al. 2009 for a summary of determinations), although the large metallicity of the cluster complicates its analysis.

In Fig. 18, we present some illustrative comparisons with model isochrones from two groups. Using distance and reddening derived from the M67 comparison above and $[\text{Fe}/\text{H}]$ equal to the most recent determination by Jacobson et al. (2008), we find adequate matches to the main sequence, but imperfect agreement with spectroscopically identified giants. De-

¹<http://www2.cadc-ccda.hia-ihp.nrc-cnrc.gc.ca/community/YorkExtinctionSolver/>

creased $[\text{Fe}/\text{H}]$ improves the agreement with the giant branch, but does not eliminate it for reasonable choices ($[\text{Fe}/\text{H}] > -0.1$). VandenBerg et al. (2010), for example, describe in detail difficulties with the color-temperature transformations that must be used to place theoretical models in the observational plane. For the Hyades, which have $[\text{Fe}/\text{H}]$ similar to NGC 7142, several transformation algorithms do a reasonable job of reproducing the main sequence. However, when it comes to the older and more metal-rich cluster NGC 6791, the authors found that the giant branch was too red when VandenBerg & Clem (2003) transformations were used (as in both sets of isochrones in Fig. 18). Given the current uncertainties in the transformations and potential problems related to the composition of super-metal rich stars (such as non-solar abundance ratios and helium abundance), we will put off further discussion of the isochrones until full analyses of the eclipsing binary stars is completed.

If the colors of main sequence stars are reliably modelled, the distance and reddening derived from the red giant clump imply an age near 3 Gyr for the cluster. Larger ages do not adequately model the bright end of the main sequence or potential subgiant branch stars ($15.5 < V < 16$ and $1 < B - V < 1.3$). This is greatly different from the age of nearly 7 Gyr derived by Janes & Hoq (2011), in spite of the fact that they derived a similar distance and reddening. It may be that their technique (which involved fitting sub-solar and solar-composition synthetic CMDs rather than super-solar ones) was affected by some of the same mismatches on the giant branch we pointed out above. If we tried to fit the color difference between the main sequence and red giant branch at the level of the turnoff with current isochrones, a much larger age would be obtained, but the red clump’s magnitude would be poorly matched.

5. Conclusions

We have conducted an extensive variability search among stars in the field of the cluster NGC 7142. Among the most important discoveries were several detached eclipsing systems near the cluster turnoff (two of which have been verified as cluster members based on radial velocities), a faint eclipsing binary with shallow eclipses indicative of a small stellar companion, and a long period variable found far to the red of the cluster giant branch. The detached eclipsing binaries allow us to put NGC 7142 on a growing list of clusters with multiple double-lined binary stars that can provide masses and radii for further tests of stellar models.

We have used the red giant clump in an attempt to derive a more reliable distance and mean reddening for the cluster. The values derived here fall at the low end of previous determinations for reddening, and at the high end for distance. Our preferred values $[E(B -$

$V) = 0.32 \pm 0.06$, $E(V - I) = 0.46$, $(m - M)_0 = 11.9 \pm 0.15]$ come from a fit of the 2MASS CMD of M67 to that of NGC 7142. With this distance, models indicate that the cluster’s age is near 3 Gyr. Future work is needed to check the agreement of theoretical models with the CMD, however, as there are lingering difficulties with color- T_{eff} transformations and with our understanding of the compositions of super-metal-rich stars.

NGC 7142 has characteristics putting it in an interesting regime. It appears to be more metal rich than the Sun or the well-studied open cluster M67, similar in metallicity to the Hyades, and more metal-poor than the very metal-rich cluster NGC 6791. As such, it can help further test metal-rich stellar models. NGC 7142’s age also is interesting — it is similar in age to M67, making it a cluster with main sequence stars that are near the transition between massive stars with convective cores and low-mass stars with radiative cores. The main difficulties in deriving accurate cluster properties are the fairly heavy reddening and field star contamination of the field. With future membership surveys (radial velocity or proper motion) or with the use of Stromgren photometry, these difficulties can be overcome.

This work has been funded through grant AST 09-08536 from the National Science Foundation to E.L.S. We would like to thank the Director of Mount Laguna Observatory (P. Etzel) for generous allocations of observing time. Infrastructure support for the observatory was generously provided by the National Science Foundation through the Program for Research and Education using Small Telescopes (PREST) under grant AST 05-19686. We would also like to thank A. Bostroem, C. Gabler, and J. B. Leep for assisting with the photometric calibration observations, and Mark Jeffries for taking some of the later time-series photometry.

The Hobby-Eberly Telescope (HET) is a joint project of the University of Texas at Austin, the Pennsylvania State University, Stanford University, Ludwig-Maximilians-Universitat Munchen, and Georg-August-Universitat Gottingen. The HET is named in honor of its principal benefactors, William P. Hobby and Robert E. Eberly. This research made use of the SIMBAD database, operated at CDS, Strasbourg, France; and the NASA/ IPAC Infrared Science Archive, which is operated by the Jet Propulsion Laboratory, California Institute of Technology, under contract with the National Aeronautics and Space Administration.

REFERENCES

- Alard, C. 2000, *A&AS*, 144, 363
- Andersen, J. 1991, *A&A Rev.*, 3, 91
- Anthony-Twarog, B. J., Deliyannis, C. P., Twarog, B. A., Cummings, J. D., & Maderak, R. M. 2010, *AJ*, 139, 2034
- Arentoft, T., et al. 2006, *Memorie della Societa Astronomica Italiana*, 77, 99
- Baldacci, L., Rizzi, L., Clementini, G., & Held, E. V. 2005, *A&A*, 431, 1189
- Cardelli, J. A., Clayton, G. C., & Mathis, J. S. 1989, *ApJ*, 345, 245
- Carraro, G., Ng, Y. K., & Portinari, L. 1998, *MNRAS*, 296, 1045
- Crinklaw, G., & Talbert, F. D. 1991, *PASP*, 103, 536
- Dotter, A., Chaboyer, B., Jevremović, D., Kostov, V., Baron, E., & Ferguson, J. W. 2008, *ApJS*, 178, 89
- Friel, E. D., Jacobson, H. R., & Pilachowski, C. A. 2010, *AJ*, 139, 1942
- Friel, E. D., Liu, T., & Janes, K. A. 1989, *PASP*, 101, 1105
- Friel, E. D., & Janes, K. A. 1993, *A&A*, 267, 75
- Friel, E. D., Janes, K. A., Tavaréz, M., et al. 2002, *AJ*, 124, 2693
- Gillon, M., et al. 2007, *A&A*, 466, 743
- Gratton, R., Bragaglia, A., Carretta, E., & Tosi, M. 2006, *ApJ*, 642, 462
- Grocholski, A. J., & Sarajedini, A. 2002, *AJ*, 123, 1603
- Grundahl, F., et al. 2006, *Memorie della Societa Astronomica Italiana*, 77, 433
- Grundahl, F., Clausen, J. V., Hardis, S., & Frandsen, S. 2008, *A&A*, 492, 171
- Hartman, J. D., Bakos, G., Stanek, K. Z., & Noyes, R. W. 2004, *AJ*, 128, 1761
- Jacobson, H. R., Friel, E. D., & Pilachowski, C. A. 2007, *AJ*, 134, 1216
- Jacobson, H. R., Friel, E. D., & Pilachowski, C. A. 2008, *AJ*, 135, 2341
- Jahn, K., Kaluzny, J., & Rucinski, S. M. 1995, *A&A*, 295, 101

- Janes, K. A., & Hoq, S. 2011, *AJ*, 141, 92
- Kaluzny, J., Pych, W., Rucinski, S. M., & Thompson, I. B. 2006, *Acta Astronomica*, 56, 237
- Kwee, K. K., & van Woerden, H. 1956, *Bull. Astron. Inst. Netherlands*, 12, 327
- Lafler, J., & Kinman, T. D. 1965, *ApJS*, 11, 216
- Lasker, B. M., Sturch, C. R., McLean, B. J., et al. 1990, *AJ*, 99, 2019
- Mathieu, R. D., van den Berg, M., Torres, G., Latham, D., Verbunt, F., & Stassun, K. 2003, *AJ*, 125, 246
- McCall, M. L. 2004, *AJ*, 128, 2144
- Meibom, S., & Mathieu, R. D. 2005, *ApJ*, 620, 970
- Montalto, M., Piotto, G., Desidera, S., et al. 2009, *A&A*, 505, 1129
- Orosz, J. A. & Hauschildt, P. H. 2000, *A&A*, 364, 265
- Piskunov, A. E., Schilbach, E., Kharchenko, N. V., Röser, S., & Scholz, R.-D. 2008, *A&A*, 477, 165
- Rose, M. B., & Hintz, E. G. 2007, *AJ*, 134, 2067
- Rucinski, S. M. 1998, *AJ*, 116, 2998
- Rucinski, S. M. & Duerbeck, H. W. 1997, *PASP*, 109, 1340
- Salaris, M., Weiss, A., & Percival, S. M. 2004, *A&A*, 414, 163
- Sandquist, E. L. 2004, *MNRAS*, 347, 101
- Sandquist, E. L., & Shetrone, M. D. 2003, *AJ*, 125, 2173
- Schiller, S. J., & Milone, E. F. 1988, *AJ*, 95, 1466
- Schlegel, D. J., Finkbeiner, D. P., & Davis, M. 1998, *ApJ*, 500, 525
- Seeberger, R., Weinberger, R., & Ziener, R. 1991, *IBVS*, 3657, 1
- Shetrone, M., et al. 2007, *PASP*, 119, 556
- Skrutskie, M. F., Cutri, R. M., Stiening, R., et al. 2006, *AJ*, 131, 1163
- Southworth, J., Maxted, P. F. L., & Smalley, B. 2004, *MNRAS*, 349, 547

- Southworth, J., & Clausen, J. V. 2006, *Ap&SS*, 304, 199
- Stetson, P. B. 2000, *PASP*, 112, 925
- Talamantes, A., Sandquist, E. L., Clem, J. L., Robb, R. M., Balam, D. D., & Shetrone, M. 2010, *AJ*, 140, 1268
- Taylor, B. J. 2007, *AJ*, 133, 370
- Thompson, I. B., Kaluzny, J., Pych, W., Burley, G., Krzeminski, W., Paczyński, B., Persson, S. E., & Preston, G. W. 2001, *AJ*, 121, 3089
- Tull, R. G. 1998, *Proc. SPIE*, 3355, 387
- Twarog, B. A., Ashman, K. M., & Anthony-Twarog, B. J. 1997, *AJ*, 114, 2556
- Twarog, B. A., Anthony-Twarog, B. J., & De Lee, N. 2003, *AJ*, 125, 1383
- VandenBerg, D. A., Bergbusch, P. A., & Dowler, P. D. 2006, *ApJS*, 162, 375
- VandenBerg, D. A., Casagrande, L., & Stetson, P. B. 2010, *AJ*, 140, 1020
- VandenBerg, D. A., & Clem, J. L. 2003, *AJ*, 126, 778
- van den Berg, M., Stassun, K. G., Verbunt, F., & Mathieu, R. D. 2002, *A&A*, 382, 888
- van den Bergh, S., & Heeringa, R. 1970, *A&A*, 9, 209
- Zhang, X. B., Deng, L., & Lu, P. 2009, *AJ*, 138, 680

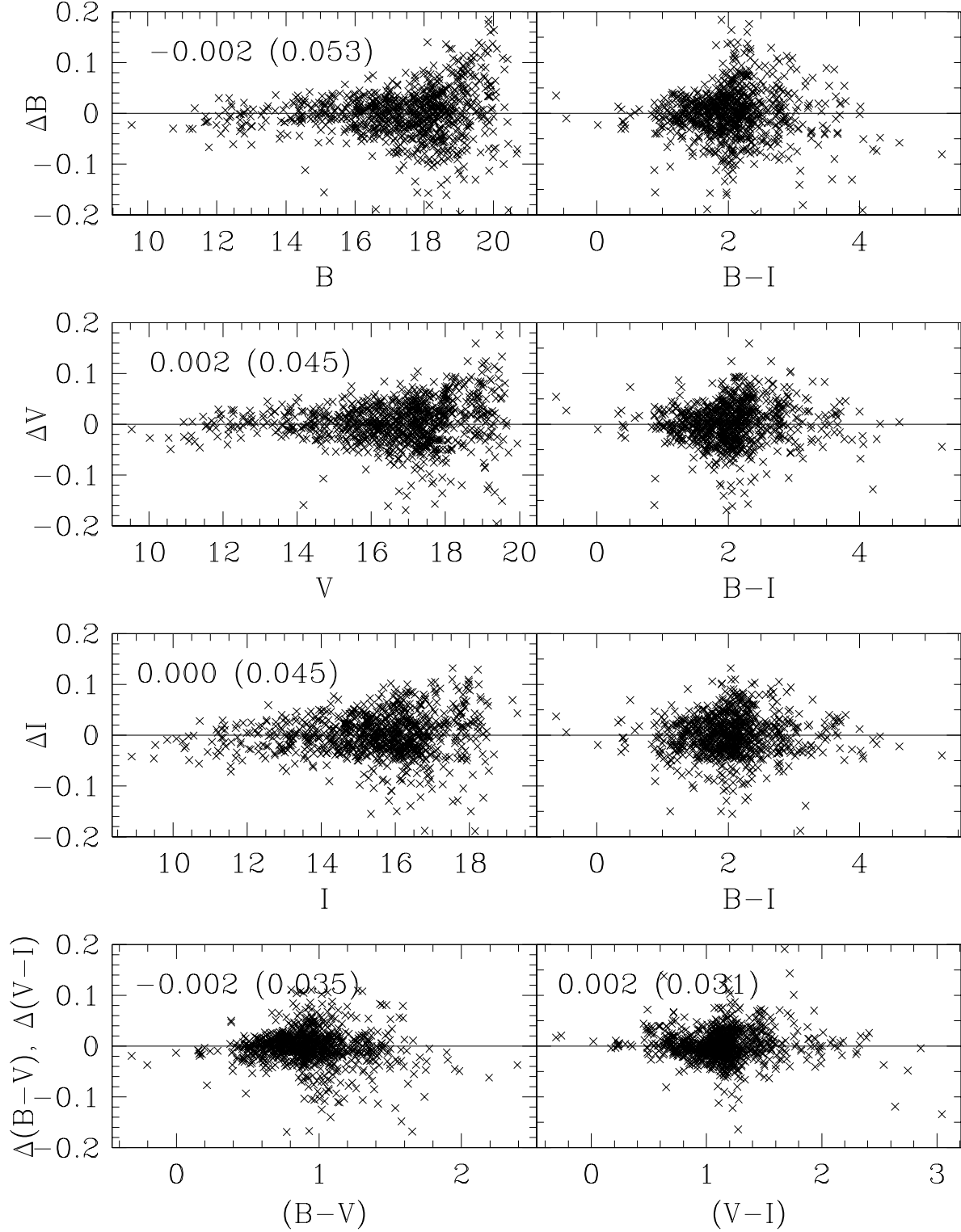


Fig. 1.— Residuals between our calibrated photometry of photometric standards and the standard magnitudes of Stetson 2000 (in the sense of this study minus Stetson’s).

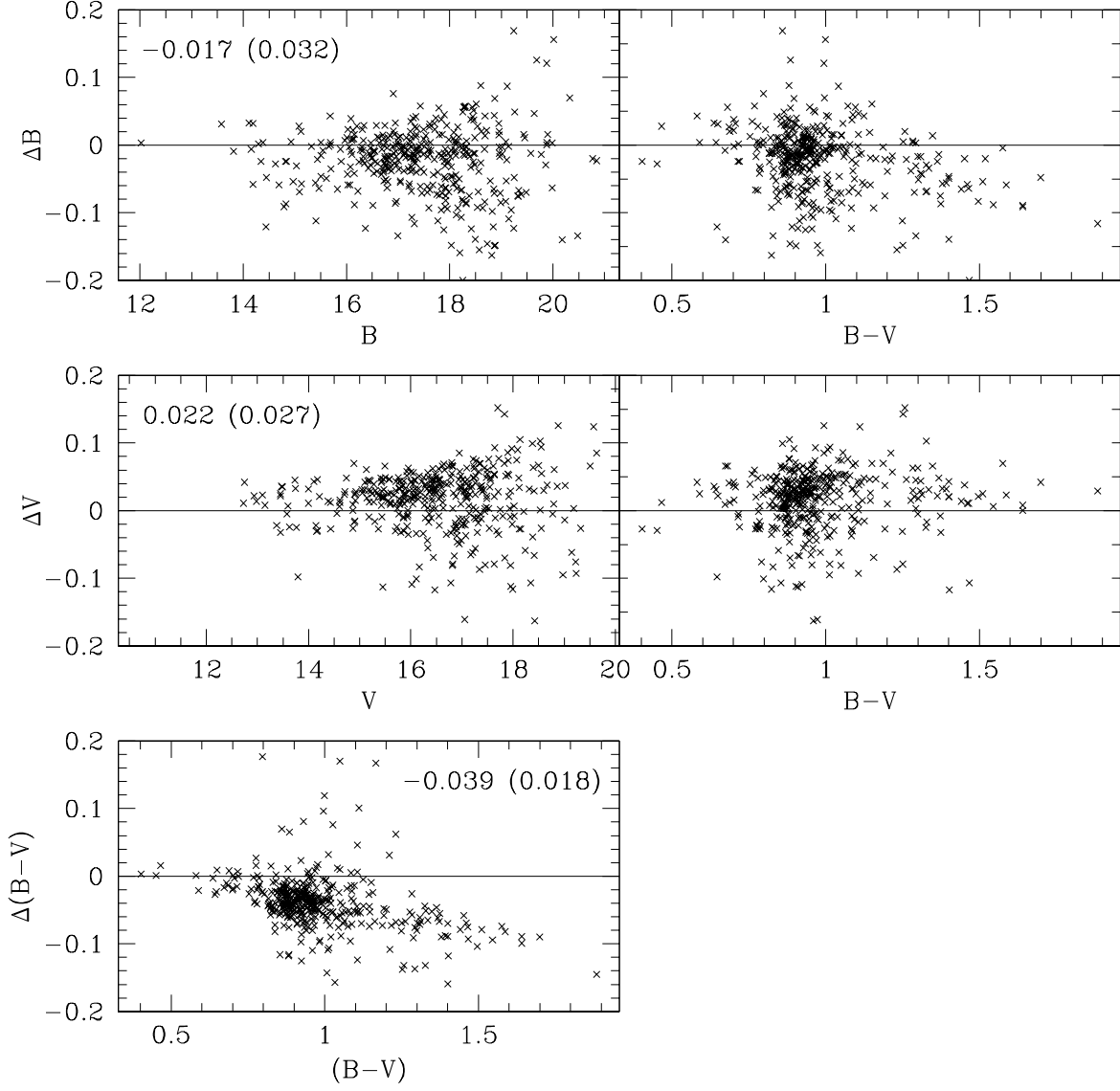


Fig. 2.— Residuals between our photometry of NGC 7142 and that of Crinklaw & Talbert (1991), in the sense of this study minus theirs. The quoted numbers are the median residual and the semi-interquartile range in B , V , and $B - V$, respectively.

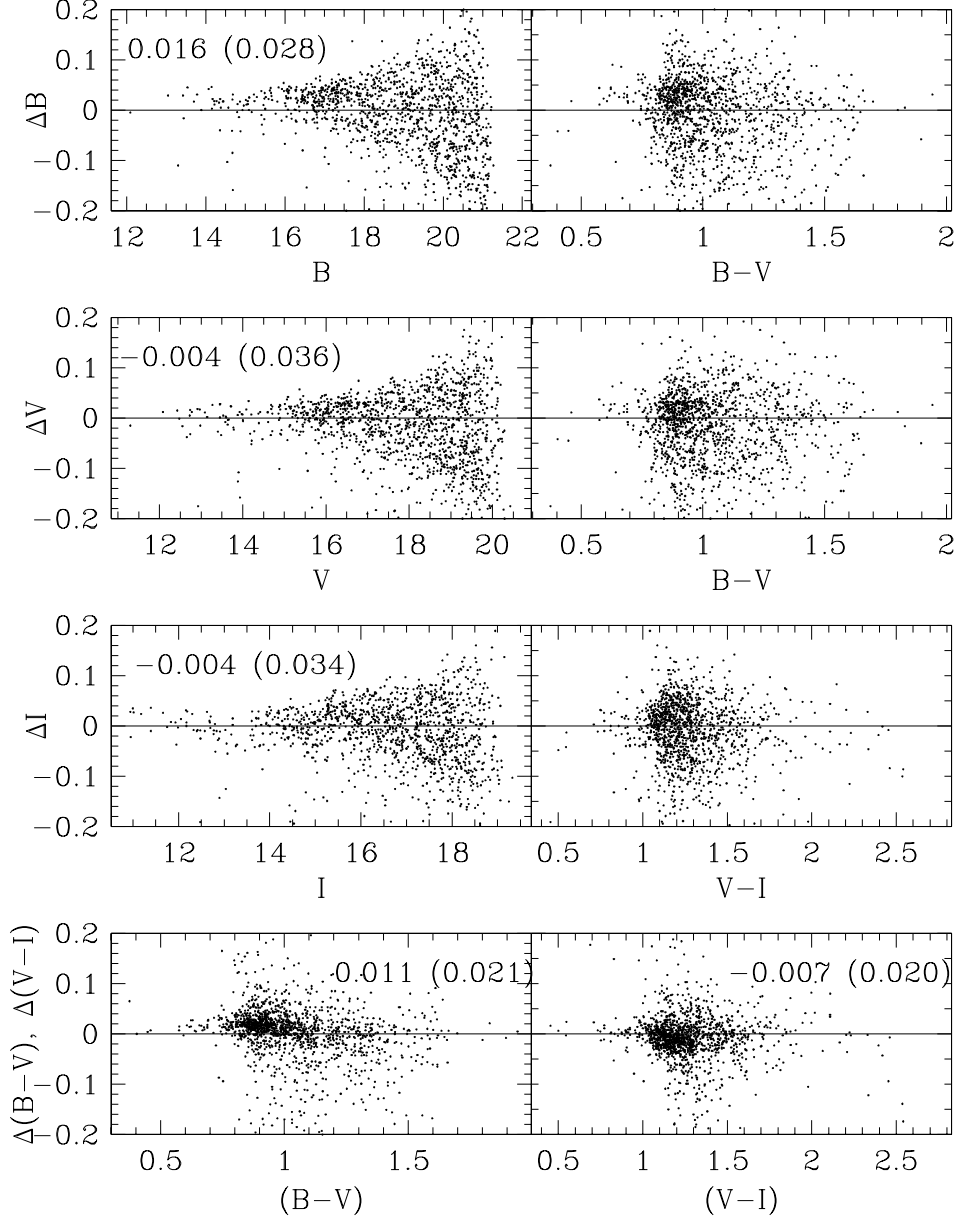


Fig. 3.— Residuals between our photometry of NGC 7142 and that of Janes & Hoq (2011), in the sense of this study minus theirs. The quoted numbers are the median residual and the semi-interquartile range. The median magnitude residuals were calculated based on stars with $B < 18$, $V < 18$, and $I < 17$, respectively.

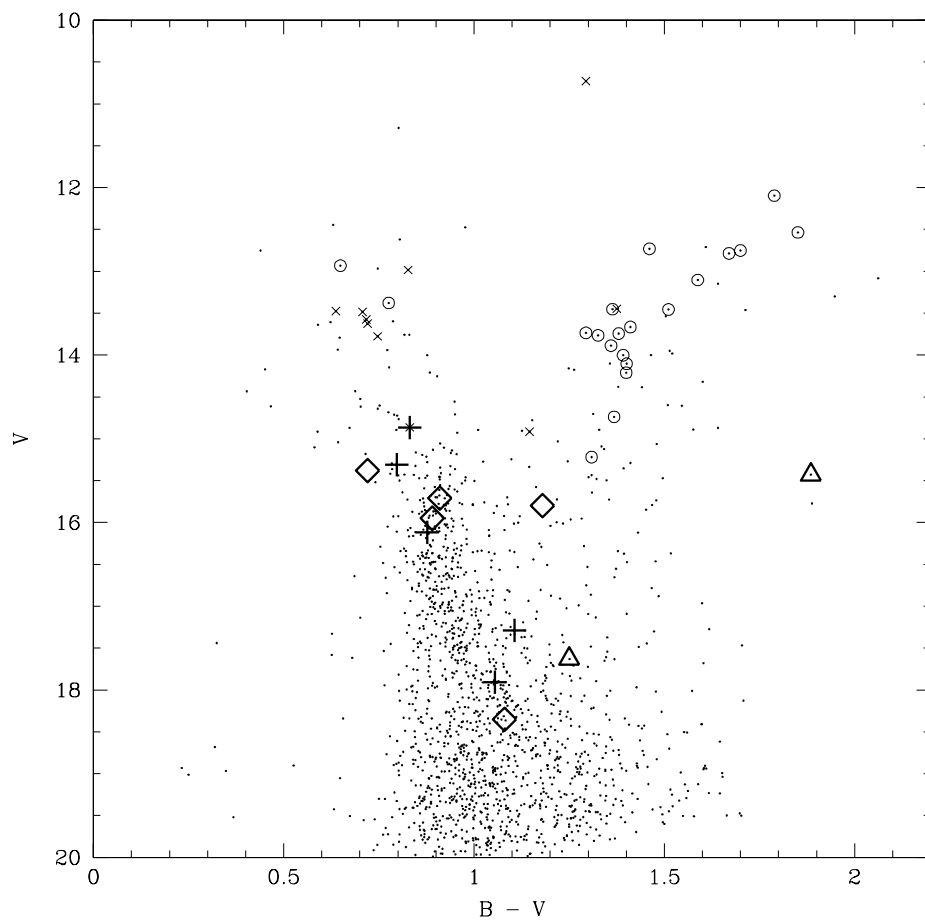


Fig. 4.— Color-magnitude diagram for NGC 7142 with variables identified. Detached eclipsing binaries are shown with crosses, contact and near contact binaries are shown with diamonds, and quasi-periodic and irregular variables are shown with triangles. Probable cluster members (identified from spectroscopic radial velocities) are shown with small open circles, and nonmembers are shown with small \times .

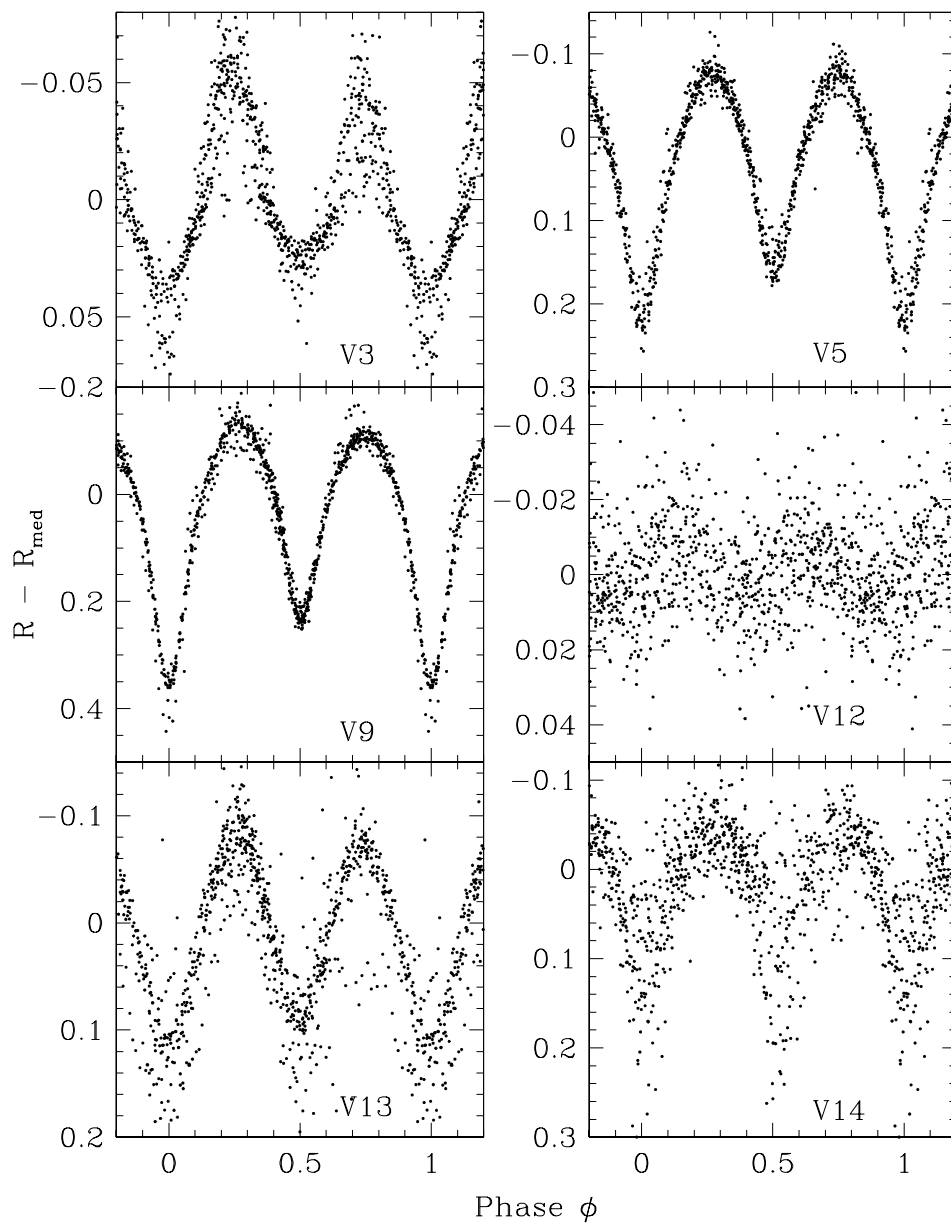


Fig. 5.— R_c phased light curves for short-period binaries V3, V5, V9, V12, V13, and V14.

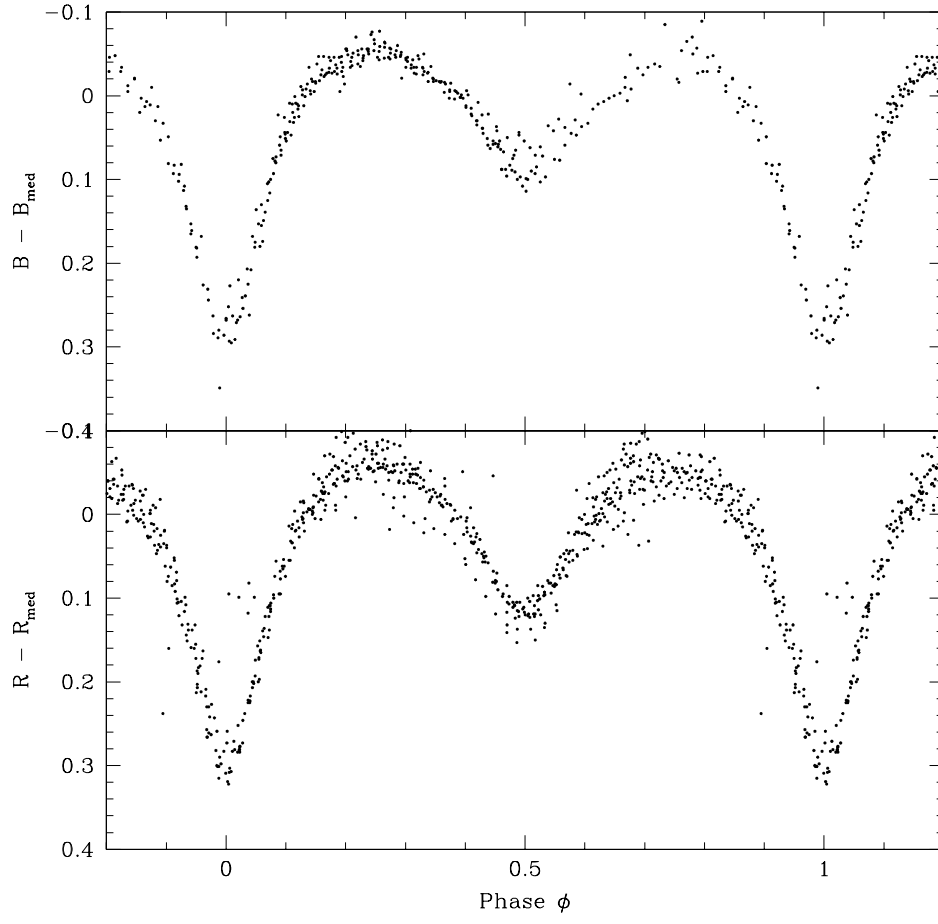


Fig. 6.— BR phased light curves for the near-contact binary V6.

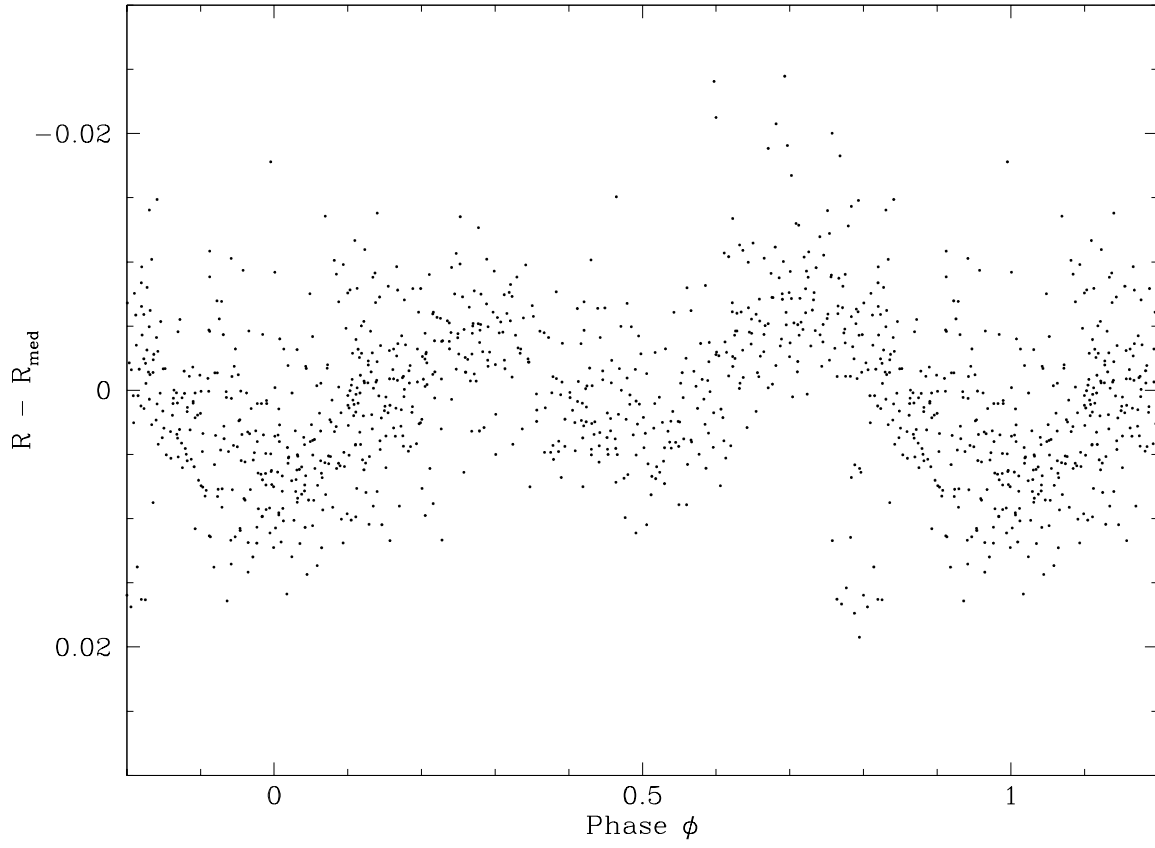


Fig. 7.— R phased light curve for the probable contact binary V7.

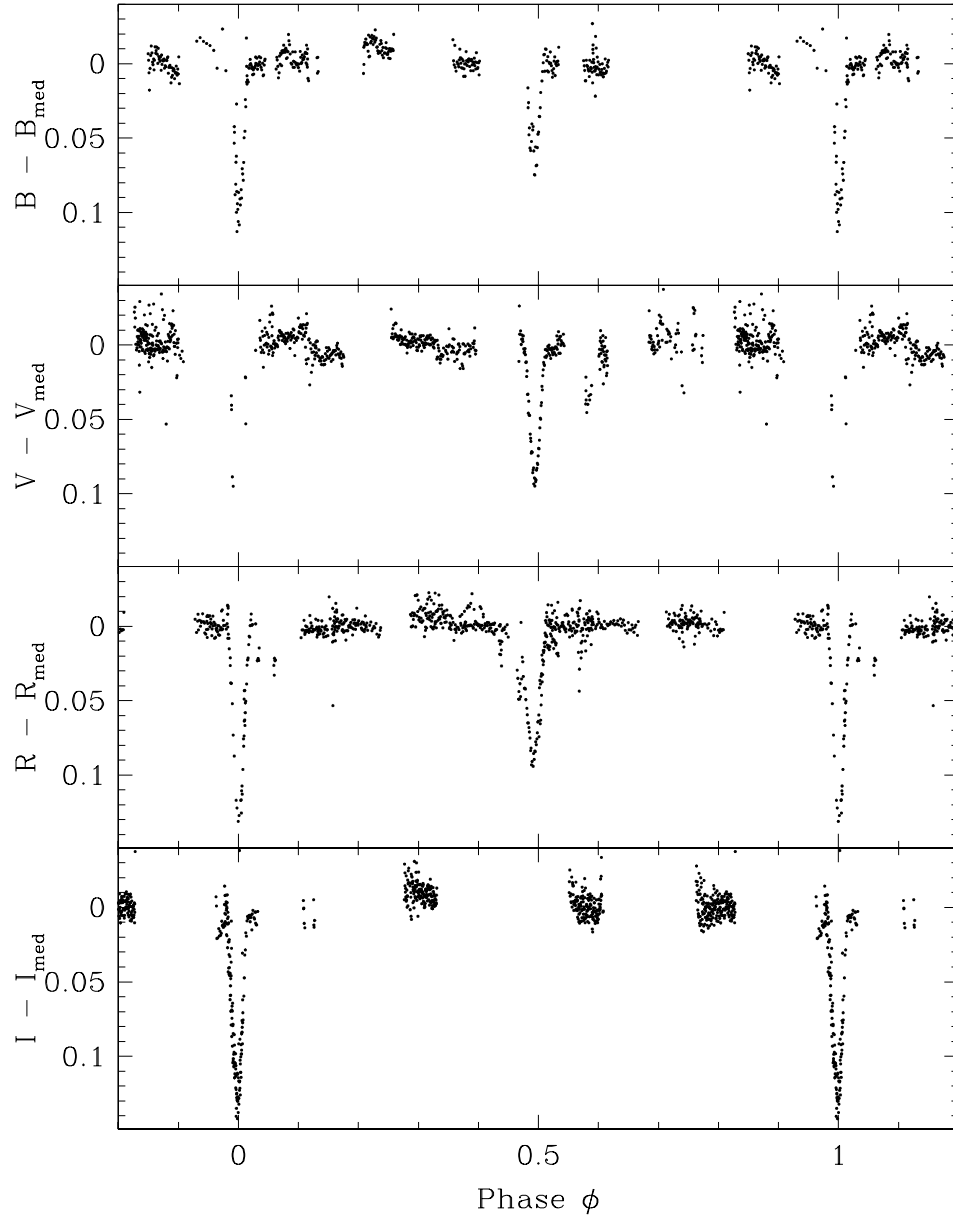


Fig. 8.— *BVRI* phased light curves for the detached eclipsing binary V1.

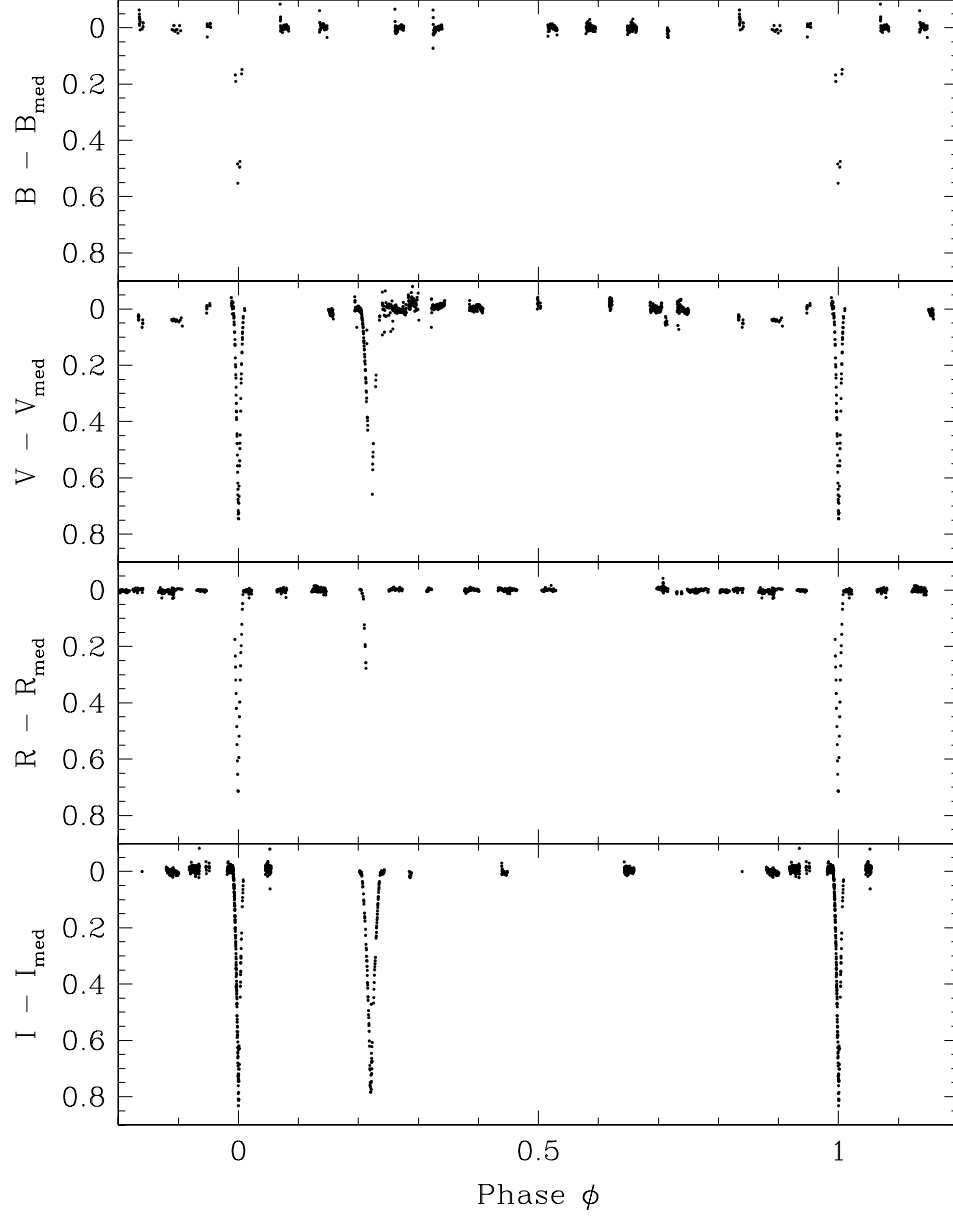


Fig. 9.— *BVRI* phased light curves for the detached eclipsing binary V2 near its eclipses. Note the longer duration of the secondary eclipse, and its displacement from a phase of 0.5.

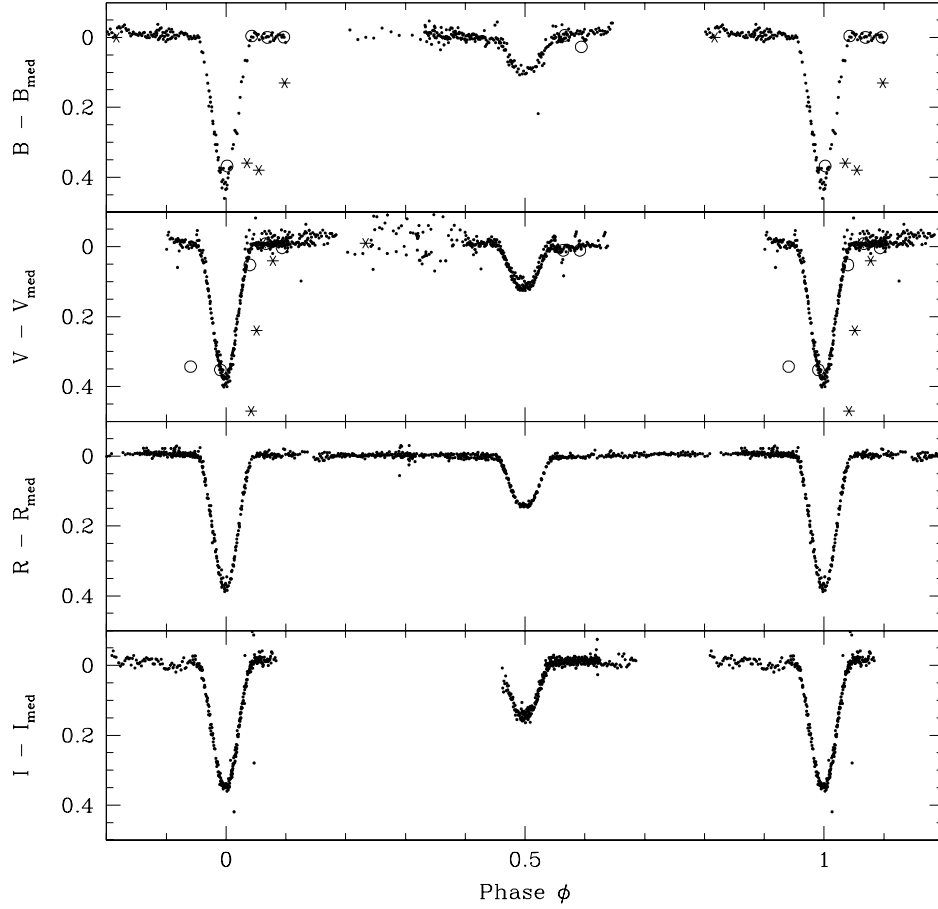


Fig. 10.— *BVRI* phased light curves for the detached eclipsing binary V375 Cep. Open circles indicate measurement made by Crinklaw & Talbert (1991) and asterisks are measurements made by Seeberger et al. (1991) phased to our ephemeris.

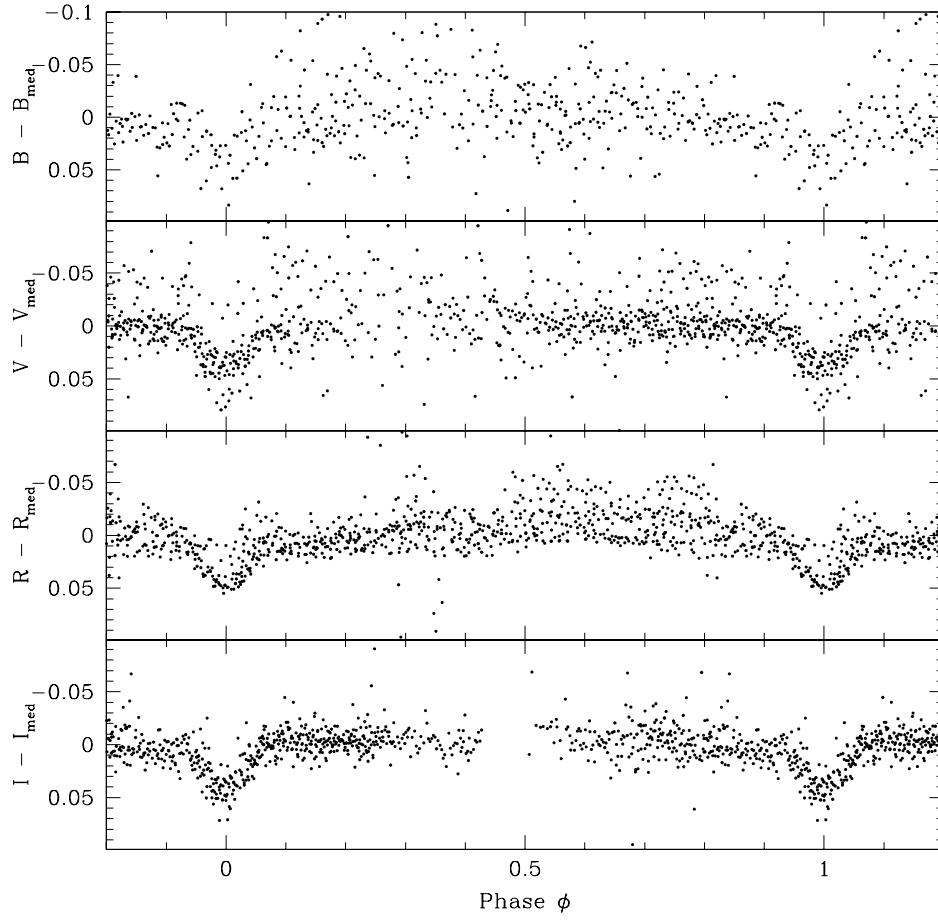


Fig. 11.— *BVRI* phased light curves for the detached eclipsing binary V8.

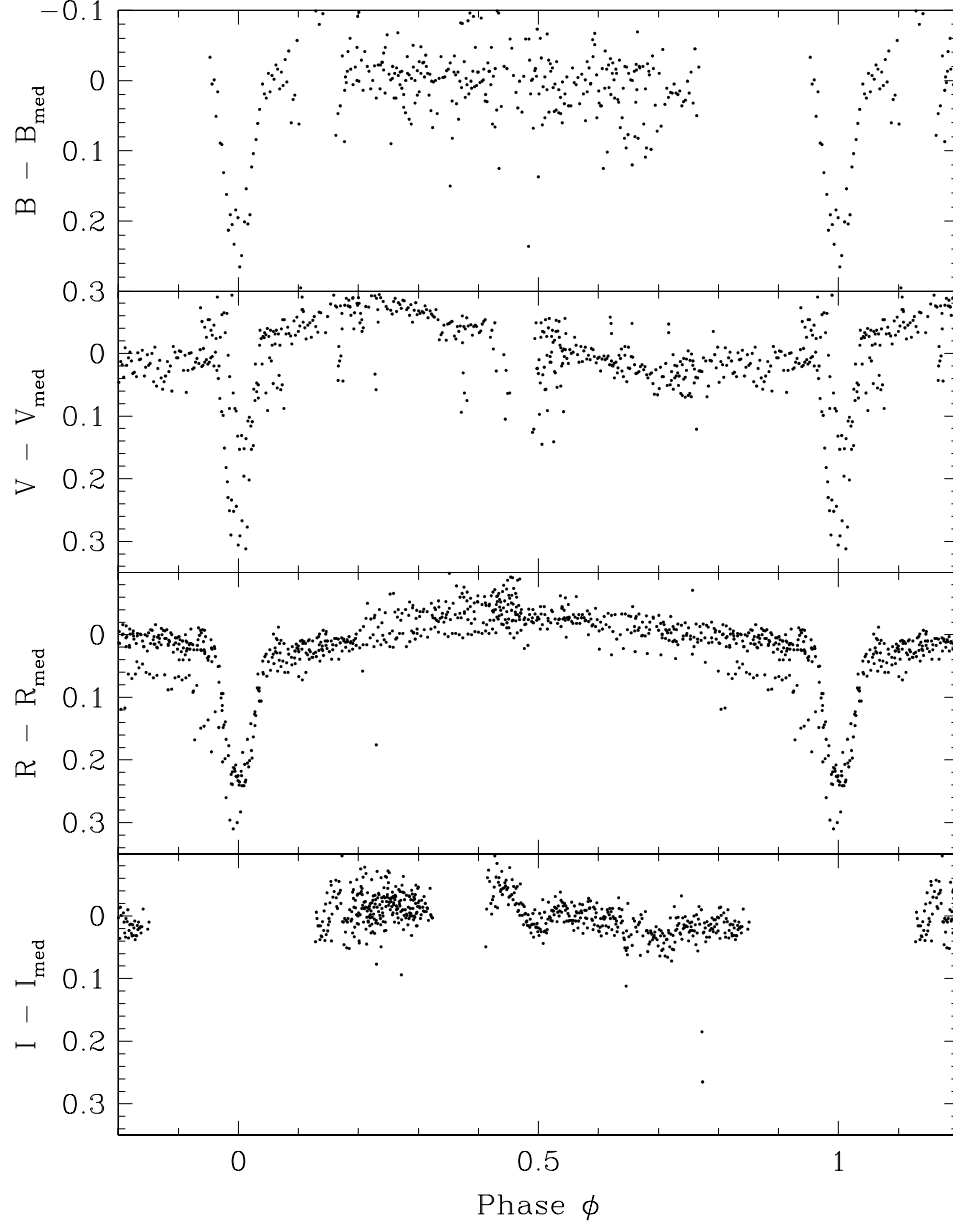


Fig. 12.— *BVRI* phased light curves for the detached eclipsing binary V11.

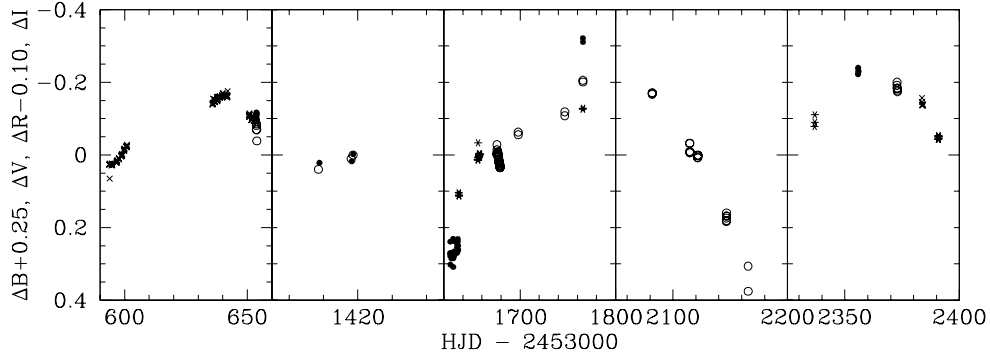


Fig. 13.— Light curves (magnitude minus the median value in each filter band) for the long-period variable V4 in B (●), V (○), R_C (×), and I_C (*). Individual points are averages of measurements made during time intervals up to 0.05 d. Measurements in B and R_C have been shifted to bring them into approximate agreement with V measurements on HJDs 2454419 and 2453653, respectively.

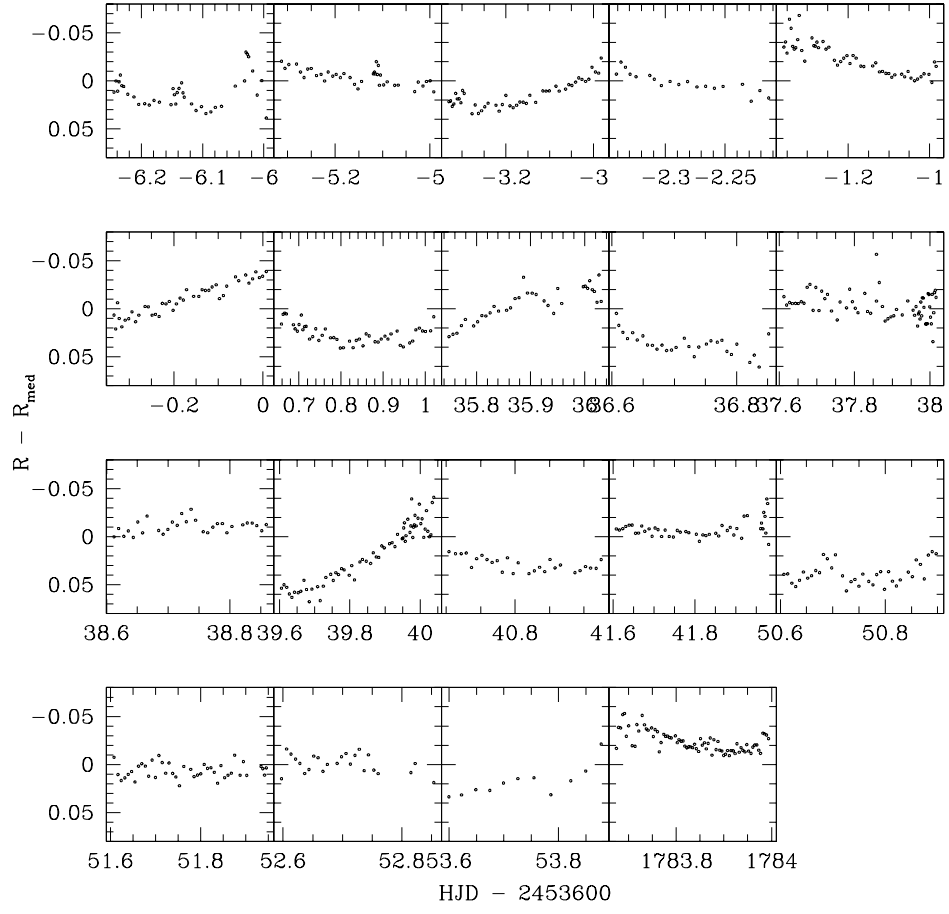


Fig. 14.— R light curves for the quasiperiodic variable V10.

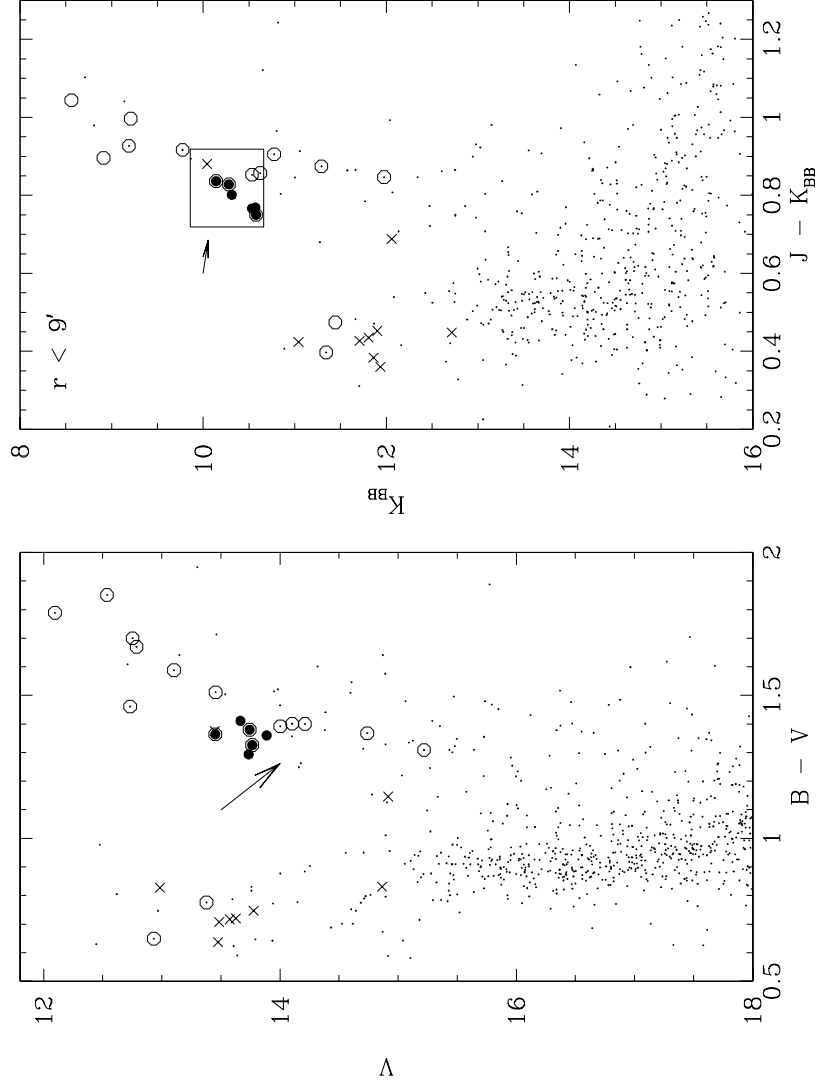


Fig. 15.— Optical (from the current study) and infrared (2MASS) CMDs for NGC 7142. Red clump candidates are identified with \bullet , likely spectroscopic cluster members are shown with \circ , and likely nonmembers are shown with \times . The box shows a Grocholski & Sarajedini (2002) red clump selection box shifted according to Janes & Hoq (2011) values for reddening and distance modulus. Reddening vectors are also shown, with lengths for both corresponding to $A_V = 0.5$ mag.

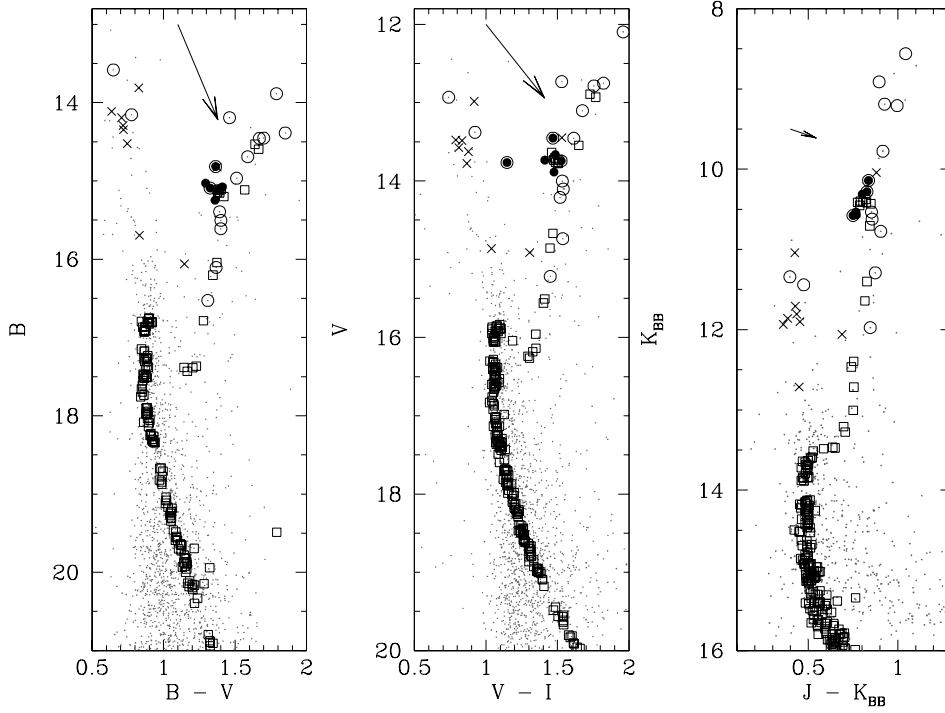


Fig. 16.— Comparison of NGC 7142 photometry with likely single-star members of M67 (\square ; Sandquist 2004). Other symbols have the same meaning as in Fig. 15. The photometry for M67 has been shifted in color to bring red clump stars into agreement in $V - I$, and the implied $E(V - I)$ was used to compute reddenings and extinctions in other filters according to the method of McCall (2004). Reddening vectors are shown in each diagram.

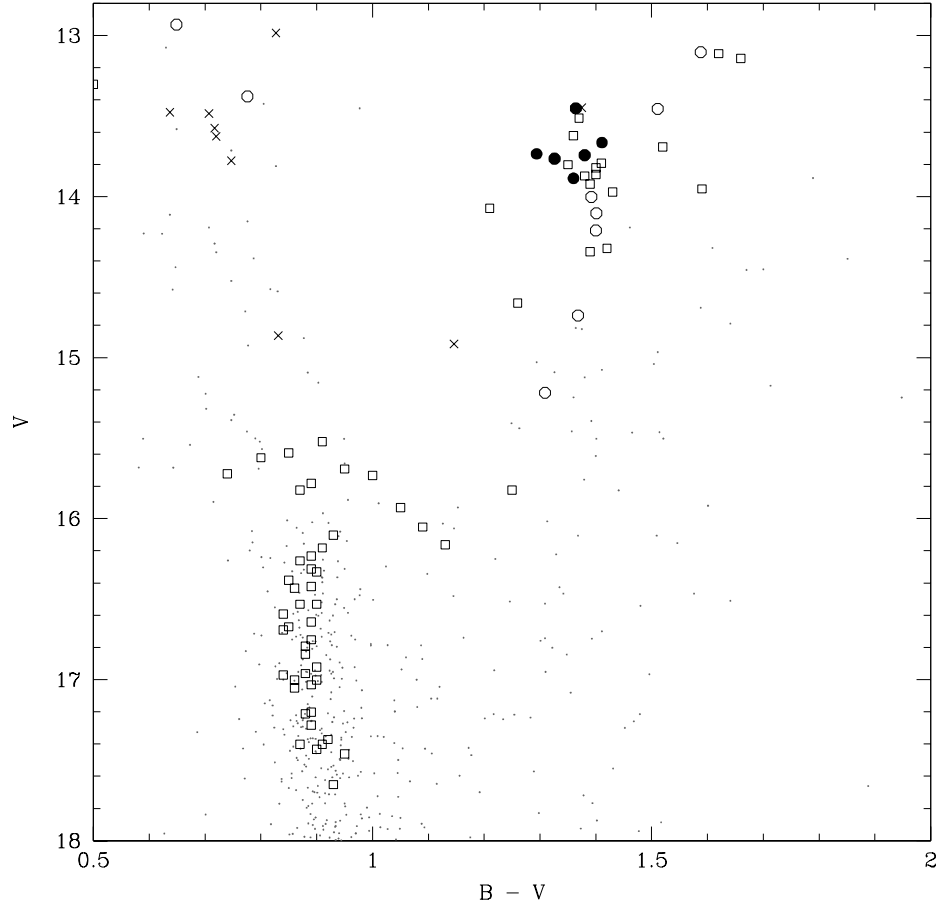


Fig. 17.— Comparison of NGC 7142 photometry with likely single-star members of NGC 6253 (\square ; Twarog et al. 2003). Other symbols have the same meaning as in Fig. 15. The photometry for NGC 6253 has been shifted in color to bring red clump and giant stars into agreement.

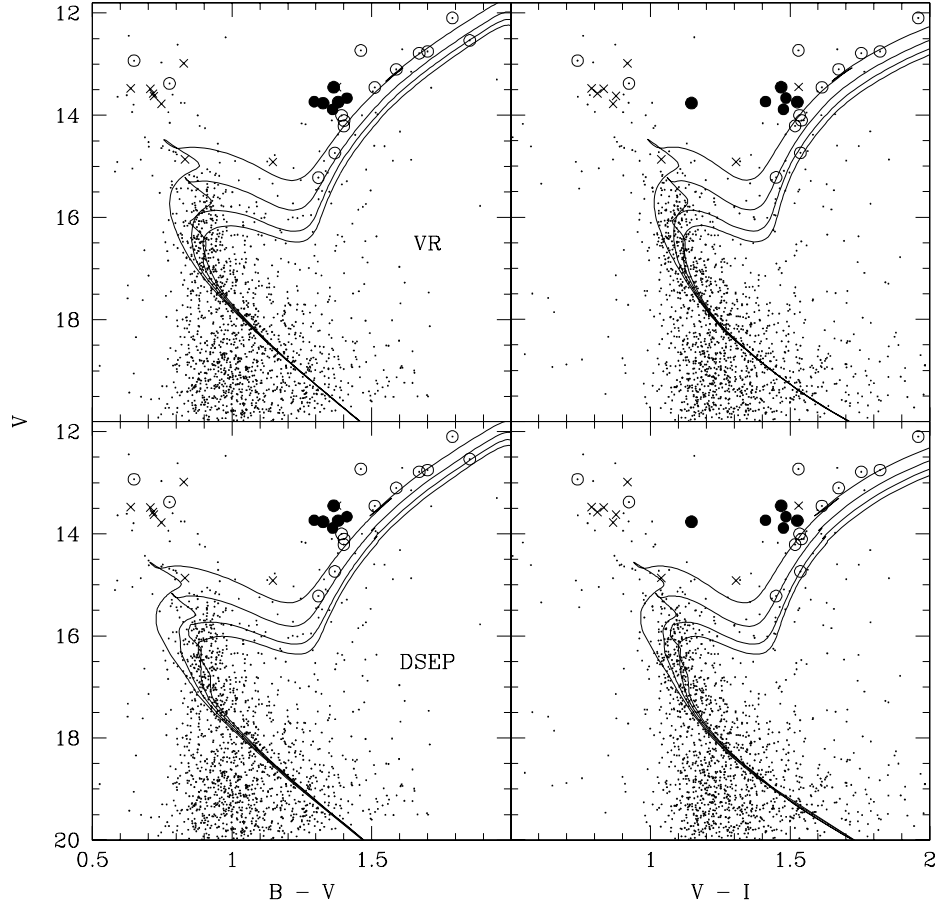


Fig. 18.— A comparison of the BVI CMDs with Victoria-Regina (VandenBerg et al. 2006) and DSEP (Dotter et al. 2008) isochrones for 2, 3, 4, and 5 Gyr in age. In both cases, $(m - M)_0 = 11.9$, $E(B - V) = 0.32$, $E(V - I) = 0.46$, and $[\text{Fe}/\text{H}] \approx +0.13$.

Table 1. Photometry at Mount Laguna Observatory

Date	Filters	mJD Start ^a	N	Date	Filters	mJD Start ^a	N
Aug. 10, 2005	R	3593.755	44	Jul. 7, 2008	I_c	4655.698	158
Aug. 11, 2005	R	3594.687	39	Jul. 8, 2008	I_c	4656.686	204
Aug. 13, 2005	R	3596.670	46	Jul. 9, 2008	I_c	4657.684	96
Aug. 14, 2005	R	3597.659	19	Jul. 27, 2008	V	4675.660	97
Aug. 15, 2005	R	3598.642	50	Jul. 28, 2008	V	4676.655	103
Aug. 16, 2005	R	3599.666	42	Jul. 29, 2008	V	4677.658	105
Aug. 17, 2005	R	3600.659	48	Jul. 31, 2008	V	4678.653	107
Sep. 21, 2005	R	3635.749	40	Aug. 18, 2008	V	4697.952	34
Sep. 22, 2005	R	3636.607	32	Oct. 6, 2008	VR_K	4746.674	11,10
Sep. 23, 2005	R	3637.613	68	Oct. 25, 2008	BVI_C	4765.686	9,8,11
Sep. 24, 2005	R	3638.612	30	Sep. 6, 2009	V	5081.895	31
Sep. 25, 2005	R	3639.605	68	Oct. 9, 2009	V	5114.592	41
Sep. 26, 2005	R	3640.704	28	Oct. 16, 2009	V	5121.578	66
Sep. 27, 2005	R	3641.608	48	Nov. 10, 2009	V	5146.575	52
Oct. 6, 2005	R	3650.607	38	Nov. 29, 2009	V	5165.590	13
Oct. 7, 2005	R	3651.608	46	May 19, 2010	I_C	5336.815	37
Oct. 8, 2005	R	3652.597	33	Jun. 7, 2010	B	5355.742	55
Oct. 9, 2005	BVR	3653.600	11,11,11	Jun. 24, 2010	V	5372.709	68
Nov. 12, 2007	BVR_K	4417.703	11,16,10	Jul. 5, 2010	R	5383.674	76
Nov. 14, 2007	BVR_K	4419.612	13,11,11	Jul. 12, 2010	I_C	5390.669	75
Jun. 8, 2008	B	4626.780	55	Aug. 2, 2010	VI_C	5411.665	12,61
Jun. 9, 2008	B	4627.796	50	Aug. 3, 2010	I_C	5412.660	11
Jun. 11, 2008	B	4629.764	57	Aug. 14, 2010	V	5423.686	18
Jun. 12, 2008	B	4630.753	60	Nov. 16, 2010	VI_C	5517.570	70,5
Jun. 15, 2008	B	4633.746	60	Jun. 23, 2011	I_C	5736.721	48
Jun. 16, 2008	B	4634.747	57	Jul. 12, 2011	RI_C	5755.670	16,65
Jun. 17, 2008	I_c	4635.740	159				

$$^{\text{a}}\text{mJD} = \text{HJD} - 2450000.$$

Table 2. Systematic Radial Velocities

ID ^a	v_{CoM} (km s ⁻¹)	σ (km s ⁻¹)	N_{obs}
Variable Stars:			
V1	-17.0	1.0	3
V2	-42.1	0.6	13
V375 Cep	-49.1	1.7	21
Red Clump Stars:			
JH2222	-49.6	0.1	1
JH2288	-44.0	0.1	1
JH1003	-43.9	0.1	1

^aV: Variable star identifier, JH: identification number from Janes & Hoq (2011).

Table 3. Variable Stars Detected in the NGC 7142 Field

	CT ^a	Type ^b	RA	DEC	V	$B - V$	$V - I$	P (d)	E_0	Notes ^c
V1	395	EA	21:44:32.86	+65:45:26.3	14.864	0.831	1.039	4.6691	2453639.93	rv prob. nm
V2	18	EA	21:44:29.62	+65:48:43.9	15.310	0.797	1.010	15.6505	2453639.684	deep eclipses; eccentric; rv mem
V3	155	EW	21:45:15.16	+65:49:24.3	15.38	0.72	0.93	0.580793	2453594.80	straggler?
V4	430	LPV	21:44:55.98	+65:45:50.0	15.43	1.89	2.06			VH Y
V5	199?	EW	21:45:30.03	+65:46:42.3	15.80	1.18	1.38	0.3368235	2453596.782	nearby faint star
V6		EB	21:44:13.21	+65:45:01.3	15.71	0.91	1.15	0.441163	2453599.757	
V7	288	EW	21:45:10.77	+65:44:41.3	15.95	0.89	1.12	0.69531?		VH f
		EA	21:44:54.74	+65:43:55.3	16.115	0.877	1.080	1.909682	2454676.8071	V375 Cep; rv mem
V8		EA	21:44:35.73	+65:45:04.7	17.288	1.106	1.373	0.52730	2453596.985	triple?
V9		EW	21:44:28.44	+65:46:36.6	17.63	1.14	1.34	0.330233	2453593.918	
V10	356	Irr	21:45:40.73	+65:43:40.0	17.63	1.25	1.53			
V11		EA	21:44:17.92	+65:50:04.9	17.906	1.055	1.304	1.28629	2453598.825	
V12		EW?	21:44:55.46	+65:52:59.0	18.330	1.157	1.340	0.2938	2453636.79	
V13		EW	21:44:20.66	+65:44:59.1	18.35	1.08	1.20	0.34207	2453598.89	total eclipses, prob. nm
V14		EW	21:46:06.8	+65:52:53.6				0.29005	2453600.75	not detected in calibrating obs.

^aCT: Identification number from Crinklaw & Talbert (1991)

^bEW: eclipsing contact or near-contact binary; EB: detached eclipsing binary with stars having ellipsoidal distortions; EA: well-detached eclipsing binary; LPV: long period variable star; Irr: irregular brightness variations

^cnm: nonmember; rv mem: membership inferred from radial velocities

Table 4. Red Clump Star Candidates in the NGC 7142 Field

CT ID ^a	JH ID ^a	RA	DEC	V	$B - V$	$V - I$	K_s	$(J - K_s)$	Notes ^b
Probable Clump Stars:									
421	1065	21:45:00.73	+65:45:56.5	13.452	1.364	1.468	10.097	0.802	I; rv, abund mem
170	1519	21:45:20.43	+65:48:31.0	13.743	1.380	1.526	10.237	0.794	O,rv mem?
203	1767	21:45:32.93	+65:47:31.1	13.765	1.326	1.147	10.533	0.718	rv, abund mem;nearby star affecting phot?
	2222	21:45:57.03	+65:44:10.5	13.665	1.411	1.485	10.268	0.768	rv mem,off CT field
93	1003	21:44:57.60	+65:48:36.8	13.735	1.294	1.412	10.490	0.734	rv mem?
	2288	21:46:00.93	+65:49:06.8	13.887	1.360	1.476	10.526	0.736	rv mem?,off CT field
Probable nonmember:									
399	591	21:44:36.70	+65:43:19.1	13.448	1.375	1.531	9.998	0.845	rv nm

^aCT: Identification number from Crinklaw & Talbert (1991), JH: identification number from Janes & Hoq (2011).

^bnm: nonmember; mem: member; rv: inference from radial velocities; abund: inference from abundances

Table 5. Estimated Extinction and Reddening Values relative to M67

Quantity	Value	Quantity	Value	Quantity	Value
$\Delta E(V - I)$	0.41	$\Delta \tau_1^a$	0.335		
ΔA_B	1.22	$\Delta(B - V)$	0.28	$A_V/E(B - V)$	3.33
ΔA_V	0.94			$A_V/E(V - I)$	2.30
ΔA_{K_s}	0.11	$\Delta E(J - K_s)$	0.15	$A_{K_s}/E(J - K_s)$	0.76

^a τ_1 is the optical depth at 1 μm .